Mineralogical Magazine, February 2012, Vol. 76(1), pp. 227–253

Review

Direct observations of mineral–fluid reactions using atomic force microscopy: the specific example of calcite

E. Ruiz-Agudo[1,2] and C. V. Putnis[2,*]

[1] Department of Mineralogy and Petrology, University of Granada, Fuentenueva s/n 18071, Granada, Spain
[2] Institut für Mineralogie, University of Münster, Corrensstrasse 24, D-48149 Münster, Germany

[*Received 25 July 2011; Accepted 4 January 2012; Associate Editor: Frank Hawthorne*]

ABSTRACT

Atomic force microscopy (AFM) enables *in situ* observations of mineral–fluid reactions to be made at a nanoscale. During the past 20 years, the direct observation of mineral surfaces at molecular resolution during dissolution and growth has made significant contributions toward improvements in our understanding of the dynamics of mineral–fluid reactions at the atomic scale. Observations and kinetic measurements of dissolution and growth from AFM experiments give valuable evidence for crystal dissolution and growth mechanisms, either confirming existing models or revealing their limitations. Modifications to theories can be made in the light of experimental evidence generated by AFM. Significant changes in the kinetics and mechanisms of crystallization and dissolution processes occur when the chemical and physical parameters of solutions, including the presence of impurity molecules or background electrolytes, are altered. Calcite has received considerable attention in AFM studies due to its central role in geochemical and biomineralization processes. This review summarizes the extensive literature on the dissolution and growth of calcite that has been generated by AFM studies, including the influence of fluid characteristics such as supersaturation, solution stoichiometry, pH, temperature and the presence of impurities.

Keywords: atomic force microscopy, calcite, crystal growth, dissolution, mineral-fluid interactions, mineral surfaces, surface science.

Introduction

The invention of atomic force microscopy (AFM) by Binnig *et al*. (1986) has enabled observations of the topography of mineral surfaces to be made at a nanometre scale. The resolution normal to the surface is at an Ångstrom level in AFM because the image is formed by tracking the interatomic forces between the outer electron shells of the atoms in a very sharp probe tip and the electrons of the atoms in the sample surface. The development of AFM in liquids by Marti *et al*. (1987) opened enormous possibilities for mineral surface science, and over the past 20 years it has become a common tool for *in situ* investigations of the dynamics of mineral growth and dissolution, with numerous publications (many of which are discussed here) reporting AFM studies of mineral surfaces and reactivity (e.g. Hochella *et al*., 1990; Pina *et al*., 1998; Orme *et al*., 2001).

The AFM operates by scanning a probe tip, which is attached to a cantilever with a known spring constant, across a sample surface. The cantilever deflection is monitored using laser light, which is reflected into a split photodiode detector. The *x*, *y* and *z* movements are produced by three piezoelectrically operated scanners. The distance the z scanner moves vertically at each (*x*, *y*) data point provides a feedback loop; this information is logged by a computer to produce a topographic image of the sample surface. The imaging conditions depend greatly on the

* E-mail: putnisc@uni-muenster.de
DOI: 10.1180/minmag.2012.076.1.227

characteristics and specifications of the AFM model that is used. Atomic force microscopes can be used to study ambient and/or liquid environments. They can operate at high temperatures (mimicking hydrothermal conditions) and in atmospheres of differing compositions and humidities, producing valuable images with applications in many scientific disciplines (e.g. biological and material sciences). Using a fluid cell, processes such as mineral growth and dissolution can be observed *in situ* in real-time experiments and detailed molecular and atomic information about these processes can be obtained.

Until recently it was not possible to obtain chemical information about the surface phase(s). Technological advances reported in Sugimoto *et al*. (2007) and references therein show that the identification of individual surface atoms is possible. They describe dynamic force microscopy, which achieves atomic resolution by detecting the short-range forces associated with the onset of chemical bonding between the outermost atom of the probe tip and the surface atoms being imaged. Dynamic force spectroscopy quantifies these forces and allows identification of the type of atom under the tip. This technique is currently limited to high-vacuum conditions.

In mineral sciences, *in situ* AFM experiments allow the investigation of dislocation source activity, two- and three-dimensional surface nucleation, critical-step length, step kinetics, step roughness and impurity-step interactions (De Yoreo *et al*. 2001). They also provide real-time information on factors influencing the kinetics and mechanisms of growth and dissolution processes, such as solution composition, supersaturation, pH, alkalinity and the presence of additives and background electrolytes. A mineral dissolves in an aqueous solution if the solution is undersaturated with respect to the mineral; similarly a mineral crystallizes from an aqueous solution if the solution is supersaturated with respect to the precipitating phase. To facilitate growth on an existing mineral surface, such as calcite, supersaturated solutions are prepared containing the required ions (e.g. calcium chloride and sodium carbonate). The speciation of the ions must be calculated to determine their activity in solution and therefore the degree of supersaturation. A program such as *PHREEQC* (Parkhurst and Appelo, 1999) is required; the degree of supersaturation is given as a saturation index (*SI*), which is defined as:

$$SI = \log \Omega = \log (IAP/K_{sp}) \quad (1)$$

where Ω is the supersaturation, *IAP* is the ion activity product and K_{sp} is the solubility product. If $SI = 0$, the mineral and solution are in equilibrium, if $SI < 0$ the solution is undersaturated and if $SI > 0$ the solution is supersaturated.

Early models of crystal growth were tested by comparing macroscopic growth kinetics with the theoretical predictions for various growth mechanisms, (e.g. Chernov, 1984; Sunagawa, 1987). These classical theories and crystal-growth models can be tested by direct observation using AFM, which provides atomic-scale information about crystal growth (Pina *et al*. 1998; Rashkovich *et al*. 2006; Astilleros *et al*. 2010). This paper provides an overview of a number of AFM studies of calcite surfaces during dissolution and growth from aqueous solution. Calcite is ubiquitous in the Earths crust and its growth and dissolution has a significant effect on global CO_2 cycling. Therefore the mechanisms of calcite crystal growth and dissolution are of particular interest in understanding environmental change. Moreover, the build up of calcium carbonate scale affects many industrial processes including water treatment and heating. Many culturally valuable buildings and statues are made from marble or limestone and determining the best method of preservation requires an understanding of the surface reactivity of calcite.

An understanding of mineral-growth processes is essential to be able to predict and control crystal growth. The molecular mechanisms that govern inhibitor–mineral interaction have been the subject of considerable research, which has focused on designing molecules to control crystal growth in a predictable way (Li and Mann, 2002). Prior to the introduction of AFM, the adsorption of molecules at mineral surfaces had been investigated using bulk experiments and the processes inferred from observations (Cabrera and Vermilyea, 1958). Atomic force microscopy allows the direct observation of such processes at a molecular level. In addition to the direct knowledge of mineral growth processes, which is valuable in designing more effective crystal-growth inhibitor molecules for industrial applications, the characterization of the effect of organic molecules on mineral growth is an important step toward understanding biomineralization (Sethmann *et al*., 2005).

It is impossible to include all AFM papers on calcite surface reactions in this review, but we

hope the research that is cited will give an overview of significant breakthroughs in understanding the thermodynamics and kinetics of calcite growth and dissolution in aqueous solutions.

Calcite surface chemistry and crystal structure

Surface chemistry and crystal structure have a direct influence on the growth and dissolution behaviour of calcite, including the mechanisms by which calcite crystals incorporate and sequester trace elements. Calcite is trigonal (it crystallizes in space group $R\bar{3}c$, and the unit-cell parameters are: a = 4.989, c = 17.062). Carbonate minerals have highly variable crystal forms whose development is related to the physical and chemical characteristics of their growth environment and the detailed growth mechanism. The most widely studied calcite surfaces are the $\{10\bar{1}4\}$ rhombohedral cleavage faces. These faces contain three non-equivalent periodic bond chains (PBC) oriented along $<4\bar{2}1>$, $<\bar{4}41>$ and $<010>$ (Paquette and Reeder, 1995). The four step edges observed on $\{10\bar{1}4\}$ faces during growth and dissolution under normal conditions reflect the rhombohedral symmetry and are parallel to the $[\bar{4}41]_+$, $[48\bar{1}]_+$, $[\bar{4}41]_-$ and $[48\bar{1}]_-$ directions (Fig. 1*a*,*b*). The subscripts (+ or −) follow the convention used by Paquette and Reeder (1995). These steps are bonded by alternating Ca^{2+} and CO_3^{2-} ions. Steps parallel to a given set of PBCs are structurally non-equivalent (Liang *et al*., 1996*b*). The structurally equivalent $[\bar{4}41]_-$ and $[48\bar{1}]_-$ steps are acute and intersect the bottom of the etch pit at an angle of 78º, whereas the $[\bar{4}41]_+$ and $[48\bar{1}]_+$ steps are obtuse and intersect the bottom of the etch pit at an angle of 102º (Hay *et al*., 2003) (Fig. 1*c*).

Atomic force microscopy has been used to study the surface structure of calcite since 1992 (Hillner *et al*., 1992; Rachlin *et al*., 1992). Non-equivalent steps on $\{10\bar{1}4\}$ calcite faces show a remarkable kinetic anisotropy when spreading during growth or dissolution (e.g. Gratz *et al*., 1993; Liang *et al*., 1996*a*,*b*; Liang and Baer, 1997). The anisotropy of obtuse and acute step velocities becomes more significant with increasing temperature (Xu *et al*., 2010). As discussed below, it also varies with other solution parameters such as supersaturation, solution stoichiometry and the specific characteristics of the background electrolyte (Teng *et al*., 1999; Larsen *et al*., 2010; Stack and Gratham, 2010; Ruiz-Agudo *et al*., 2011*a*,*b*). Lateral atomic-scale resolution has been achieved in many AFM studies, allowing resolution of kinked monoatomic steps and the determination of atomic-scale periodicities (e.g. Hillner *et al*., 1992; Rachlin *et al*., 1992; Ohnesorge and Binnig, 1993). Hillner *et al*. (1992) described the atomic structure of the calcite cleavage plane as a nearly rectangular atomic array with vertical columns separated by 0.40±0.04 nm and faint corrugated horizontal rows separated by 0.46±0.04 nm. This corre-

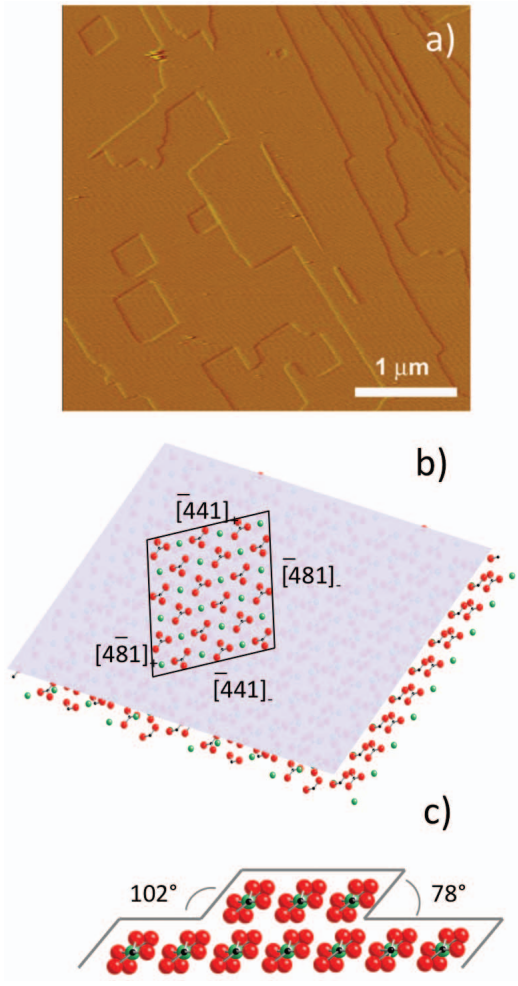

FIG. 1. (*a*) An AFM deflection image of a calcite cleavage surface upon contact with deionized water. (*b*) Sketch showing non-equivalent directions parallel to the $<\bar{4}41>$ calcite periodic bond chain. (*c*) Obtuse (+) and acute (−) steps on a calcite $\{10\bar{1}4\}$ plane.

sponds most probably to a rectangular net of calcium atoms and carbonate groups with a cell size of 0.40×0.50 nm. The near-atomic resolution images of the calcite cleavage surface obtained by Rachlin *et al*. (1992) suggest that there is minimal reconstruction of the surface. The surface cell parameters that they determined from the images in Fourier space are in good agreement with both the parameters calculated for the bulk structure and those derived from low-energy electron diffraction (LEED) images (Stipp and Hochella, 1991). Furthermore, these studies have provided evidence of the order and crystalline nature of calcite $\{10\bar{1}4\}$ surfaces in air and aqueous solutions.

The high-resolution images of these surfaces, produced by AFM, show striking features, such as the offset of alternate rows as well as pairing and alternation in the height of the rows (Stipp, 1999). These features depend systematically on the force and direction of tip scanning, and are considered to provide evidence for the presence of dissociated H_2O (OH^- and H^+) at the termination of the bulk calcite structure. Specifically, they originate due to the presence of OH groups filling the vacant sites created when calcite is cleaved along the $\{10\bar{1}4\}$ plane. Recently, experiments in a 96% ethanol–water mixture have shown that ethanol binds more strongly than water to calcite, modifying its surface reactivity and representing a barrier for solute attachment and detachment, and as a consequence affecting calcite growth and dissolution (Cooke *et al*., 2010; Sand *et al*., 2010). This observation may have important implications for biomineral growth in environments with a low water activity and a high concentration of organic molecules and is discussed later.

Dissolution reactions

The kinetics and mechanisms of calcite dissolution in aqueous solutions has attracted much attention and has been studied extensively, the primary motivation being the potential use of calcite in the large-scale geological capture and storage of CO_2. In the last two decades, an increasing number of dissolution studies have focused on direct observation and quantification of the kinetics of dissolution processes on calcite surfaces using scanning probe microscopy (e.g. Stipp *et al*., 1994; Dove and Platt, 1996; Liang *et al*., 1996*a*; Liang and Baer, 1997; McCoy and LaFemina, 1997; Lea *et al*., 2001; Morse and Arvidson, 2002; Arvidson *et al*., 2003; Bisschop *et al*., 2006). Atomic force microscopy can be used to observe dissolution processes at rates in the range from 10^{-10} to 10^{-6} mmol m^{-2} s^{-1} (Dove and Platt, 1996). Thus, AFM provides an optimal technique for the study of carbonate, and in particular calcite, reactivity. It allows direct microscale to nanoscale *in situ* observations of mineral–water reaction processes on crystal surfaces, contributing to a deeper understanding of the controls on the processes that occur at the interface between calcite and aqueous solutions. Furthermore, information from AFM experiments facilitates the interpretation of results obtained from calcite dissolution studies carried out using traditional methods (Plummer *et al*., 1978; Sjöberg and Rickard, 1984; Compton *et al*., 1989; Schott *et al*., 1989; MacInnis and Brantley, 1992; Gutjahr *et al*., 1996; Oelkers *et al*., 2011).

The role of surface defects on dissolution.

Dissolution of calcite cleavage surfaces occurs by the retreat of surface steps in certain preferred crystallographic directions. Effectively, step motion takes place by the preferential removal of the ionic species in calcite by lateral advancement of kink sites (i.e. surface sites in which the number of bonds that coordinate the ions building the crystal at that site is half that of the same ions in the bulk crystal). These steps remain straight and maintain a constant velocity during dissolution in pure solutions and at low supersaturation (Liang *et al*., 1996*b*), and are either originally present before solution exposure or created upon contact with the solution by the generation of etch pits (Fig. 1*a*). Etch pit formation is a fundamental step in the dissolution of calcite because it provides a source of step edges where the nucleation of kink sites is energetically favoured in comparison to an atomically flat surface (Liang *et al*., 1996*a*). MacInnis and Brantley (1992) noted that etch pit nucleation on calcite cleavage surfaces occurs primarily at surface defects: point defects in the case of shallow etch pits and dislocations in the case of deep etch pits (Liang *et al*., 1996). According to the stepwave dissolution model proposed by Lasaga and Luttge (2001), the kinetics of mineral dissolution is controlled by the propagation of a train of steps (stepwaves) emerging from deep etch pits nucleated at dislocations. The result of this process is a layer-by-layer removal of material from the mineral surface that leads to retreat normal to the surface (Luttge *et al*., 2003).

In this model, both the velocity and spacing of stepwaves depends on the solution supersaturation or ΔG, thus reproducing the dependence of dissolution rates on ΔG observed in macroscopic dissolution experiments.

Studies of carbonate dissolution by AFM have shown that the formation and spreading of shallow etch pits may also make an important contribution to the overall dissolution rate. As discussed in the next section, under certain conditions of supersaturation or solution composition, a high density of shallow etch pits may form on calcite surfaces. The typical maximum value of dislocation density for the (unstrained) Iceland-spar crystals commonly used in AFM dissolution experiments is ~10^6 cm^{-2} (see Bisschop *et al*., 2006, and references therein). This value is in agreement with the density of deep etch pits observed in AFM studies (e.g. Ruiz-Agudo *et al*., 2009). The average density of point defects of Iceland spar is estimated to be ~10^5 cm^{-2} (MacInnis and Brantley, 1992). However, the value of etch pit density observed for Iceland-spar dissolution at very low supersaturations is ~10^8 cm^{-2}, which is two orders of magnitude greater than the estimated total defect density (Teng, 2004; Ruiz-Agudo *et al*., 2009). Therefore, a significant proportion of the observed etch pits must have nucleated in defect-free areas of the crystal surface. The coalescence of these shallow etch pits is generally fast and results in the removal of a whole surface layer before a stepwave front, that originated at a deep etch pit, has propagated over the entire surface. This has also been observed at circumneutral pH values in far from the equilibrium conditions in the case of dolomite dissolution (Ruiz-Agudo *et al*., 2011*c*; Urosevic *et al*., 2012).

Mechanisms of calcite dissolution in aqueous solution: dependence on distance from equilibrium

Most calcite dissolution studies have focused on processes occurring in systems that are far from equilibrium, with the intention of gaining fundamental knowledge about the kinetics of these processes. Numerous AFM studies show that calcite dissolution at very high undersaturation occurs mainly by the nucleation and spreading of rhombohedral etch pits (Fig. 2). Relatively few studies have addressed calcite dissolution processes in near-equilibrium conditions. Teng (2004) studied the control that the saturation state exerted on the mechanisms of calcite dissolution in highly undersaturated to near-equilibrium aqueous solutions. He noted that etch pits did not form if conditions were close to equilibrium but they nucleated rapidly if conditions were far from equilibrium, and suggested that calcite dissolution takes place by three different mechanisms, depending on the degree of undersaturation of the solution. Dissolution at pre-existing steps is the main mechanism close to equilibrium;

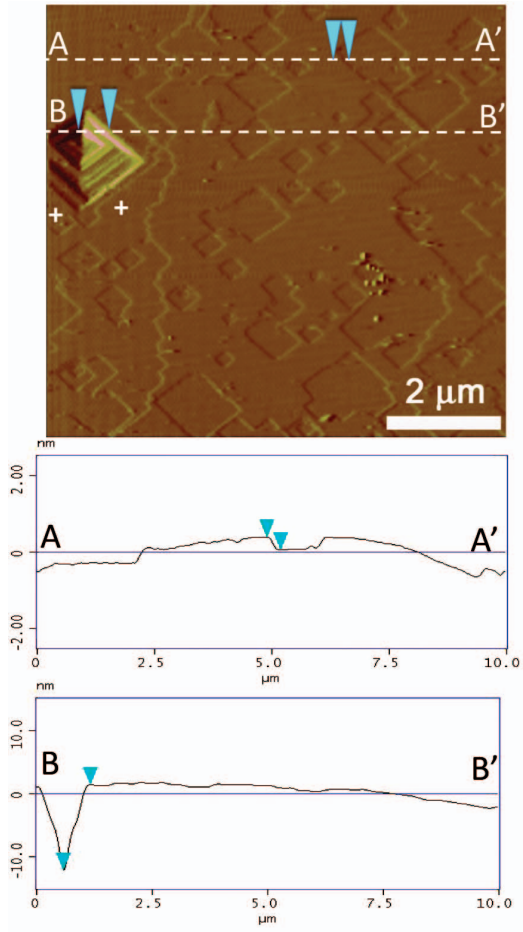

FIG. 2. Deep (dislocation-nucleated) and shallow etch pits formed on calcite cleavage surfaces upon contact with a highly undersaturated solution. Atomic force microscopy deflection image and vertical profiles: (*a*) AA′ (shallow etch pit) (*b*) BB′ (deep etch pit). The vertical distance between points marked with arrows in AA' and BB' profiles is 0.3 (~1 unit cell) and 13.6 (~45 unit cells) nm, respectively.

defect-assisted dissolution becomes increasingly important at medium undersaturation; at high undersaturation, etch pit nucleation on defect-free surfaces becomes the dominant mechanism due to the reduction in the energy barrier for unassisted pit nucleation. Under these conditions, dislocation-induced dissolution plays a secondary role. These three main mechanisms were also observed by Xu *et al*., (2010), who also reported increased step velocities with increasing undersaturation. Furthermore, they found that, at supersaturation values (Ω) above 0.02, etch pits had near-triangular shapes as a result of the development of a new step that cuts across the two negative (acute) steps.

The transition between different dissolution mechanisms occurs at two critical saturation states: Ω_c, the critical supersaturation at which the barrier for pit nucleation at dislocations disappears and Ω_{max}, the saturation state at which unassisted pit formation begins. Teng (2004) reported Ω_c values of 0.541–0.410 and an Ω_{max} of 0.007 for dissolution at room temperature, and Xu *et al*. (2010) estimated an Ω_c value of 0.3 at temperatures ranging from 50–70ºC. The existence of an Ω_c value is in agreement with the dislocation theory, but not the occurrence of a supersaturation threshold for unassisted pit nucleation. This saturation-dependence of the dissolution mechanism helps in understanding of some well known features of the kinetics of dissolution processes, such as the weak dependence of dissolution rate on dislocation density in distilled water and the approximately constant dissolution rates measured both near and far from equilibrium (Teng, 2004).

Kinetics of calcite dissolution as measured by AFM.

As well as mechanistic information on growth and dissolution, AFM provides important kinetic information on mineral–fluid interactions (Fig. 3). Mineral dissolution rates can be controlled by the kinetics of the surface reaction and/or the mass transport of the dissolved species from the crystal surface. The slowest of these processes controls the dissolution rate and is the rate-determining step. Mass transport is commonly important during calcite dissolution at acid pH, whereas surface reaction kinetics generally control calcite dissolution in far-from-equilibrium (i.e. highly undersaturated) conditions at circumneutral or slightly alkaline pH values

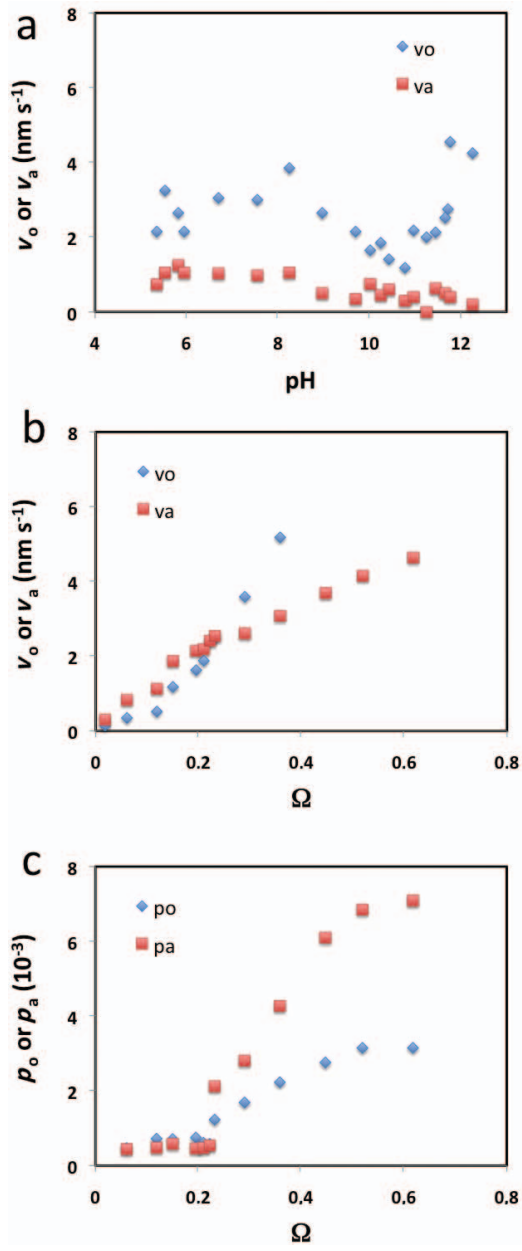

FIG. 3. Quantitative kinetic data obtained from AFM images in (*a*) calcite dissolution and (*b*,*c*) growth experiments: velocity of obtuse (v_o) and acute (v_a) step spreading (*a*) as a function of pH; (*b*) as a function of solution supersaturation; and (*c*) as a function of obtuse (p_o) and acute (p_a) step density. Plots from data in Shiraki *et al*. (2000) (*a*) and Teng *et al*. (2000) (*b*,*c*).

(Arvidson *et al*., 2003). Calcite dissolution was considered to be diffusion controlled at pH <4.4 and governed by the surface reactivity at pH >5.3 by Shiraki *et al*. (2000). However, De Giudici (2002) reported a pH value of 2.7 for the transition between surface-controlled and diffusion-controlled regimes. This author suggested that even at this low pH, the kinetic regime can be controlled locally by diffusion in areas of high step density, whereas in other reactive areas, such as shallow etch pits, the kinetics is controlled by surface reactivity, giving rise to the mixed-controlled regime observed in macroscopic experiments (Plummer *et al*., 1978). Macroscopic studies established that the change from the surface-controlled regime to the diffusion-controlled regime occurs at pH <4 (e.g. Plummer *et al*., 1978; Sjöberg and Rickard, 1984; Compton and Unwin, 1990). During dissolution, the local pH of the solution may vary, and there may be a gradient in pH from the calcite surface into the fluid. The maintenance of this gradient would then also depend on the flow rate. From an AFM operational point of view, flow rates above 9 ml h^{-1} ensure that the dissolution process is surface controlled at slightly alkaline pH values (Liang *et al*., 1996a); however, for pH values of <5.3, flow rates greater than 29 ml h^{-1} are required for the velocity of step retreat to be independent of flow rate (at room T and pCO_2 ~$10^{-3.5}$ atm; Shiraki *et al*., 2000).

Dissolution rates in AFM studies can be inferred from the absolute rates of non-equivalent step propagation (i.e. v_+ and v_-, the retreat velocities of obtuse and acute steps, respectively), which are estimated by measuring the distances of the obtuse and acute step edges from fixed reference points in sequential images scanned in the same direction (e.g. Teng, 2004; Xu and Higgins, 2011). These measurements are sensitive to sample drift, and therefore dissolution rates are more commonly reported based on the etch pit spreading rate, v_{sum}, which is defined as $v_{sum} = (v_+ + v_-)$ and calculated by measuring the length increase per unit time of opposite parallel steps in sequential images (Liang *et al*., 1996*b*). The ratio v_+/v_- can be obtained by measuring the slopes of steep pits as follows (Duckworth and Martin, 2004): $v_+/v_- = m_+/m_-$ were m_+ and m_- are the slopes of the obtuse and acute pit walls, respectively. If v_{sum} and m_+/m_- are known, v_+ and v_- are readily calculable.

Many AFM studies have reported step velocities on the calcite cleavage plane during dissolution. Hillner *et al*. (1992) measured etch pit expansion rates in a 0.015 M NaOH solution (with a calculated pH of 12.1) of 1.1 to 1.6 nm s^{-1}. Values for v_{sum} of 4.2 and 4.9 nm s^{-1} at pH 9 were found by Liang and coworkers (Liang *et al*., 1996*b*; Liang and Baer, 1997). These authors reported a constant value for v_+/v_- of 2.3±0.2, giving $v_- = 1.3-1.5$ nm s^{-1} and $v_+ = 2.9-3.4$ nm s^{-1}. Later, Jordan and Rammensee (1998) measured v_{sum} at 3.0 nm s^{-1} with $v_+ = 2.5\pm0.5$ nm s^{-1} and $v_- = 0.5\pm0.2$ nm s^{-1} in deionized water at pH 5.6 (at pCO_2 ~$10^{-3.5}$ atm). These few examples illustrate the high sensitivity of the step retreat velocity to experimental conditions, in particular, pH. Shiraki *et al*. (2000) investigated the effect of pH on the velocity of obtuse and acute steps systematically. The obtuse step-spreading rate increased with the pH value between 6 and 8.5, then decreased between 8.5 and 10.8, where a minimum of 1.1 nm s^{-1} was measured. In contrast, the acute-step velocity decreased with pH up to 10.8, and remained constant at higher values (Fig. 3*a*).

Temperature is expected to have a significant effect on step spreading rates. However, few studies have dealt with the kinetics of calcite step advancement at different temperatures. At high undersaturation, AFM calcite dissolution studies report similar activation energies for both obtuse and acute steps (57–59 kJ mol^{-1}; Liang and Baer, 1997; Liang *et al*., 1996*a*) (between 22 and 50ºC). In conditions close to equilibrium and at higher temperatures (50–70ºC), Xu *et al*. (2010) obtained lower activation energies of 25±6 kJ mol^{-1} for the obtuse and 14±13 kJ mol^{-1} for the acute steps. The origin of this discrepancy between values estimated in different AFM studies remains unclear, but it may be related to the increasing influence of the backward reaction on step velocities (and therefore, the variation of the kinetic coefficients) with increasing supersaturation (Xu *et al*., 2010) or to changes in the hydration of surface steps with increasing solution temperature.

Overall dissolution rates, R_{AFM} (in mol cm^{-2} s^{-1}) can be determined directly from sequences of AFM images by measuring the volume increase of etch pits, ΔV, over a given area of calcite in a given time. During dissolution, etch pits deepen and widen, thus changing their height and lateral dimensions. If there are N_{pit} etch pits per unit area of surface and ΔV is the volume loss in the time between two sequential images $t_2 - t_1$ for a rhombohedral etch pit, the

overall dissolution rate can be calculated using the equation:

$$R_{\mathrm{AFM}} = \frac{(\Delta V)N_{\mathrm{pit}}}{V_{\mathrm{m}}(t_2 - t_1)} \quad (2)$$

where V_{m} is the molar volume of the mineral. Images of sufficient size are required if N_{pit} values are to be representative. This procedure allows the calculation of surface-specific dissolution rates from AFM measurements (Dove and Platt, 1996; Shiraki *et al*., 2000; Duckworth and Martin, 2004). However, there are some limitations. Due to the absence of a reference (unreacted) surface in AFM experiments, the measurements are only realistic in cases where the layer removal rate is slower than the increase in etch-pit depth. A comprehensive review of published calcite dissolution data is provided in figure 1 of Arvidson *et al*. (2003). In general, the overall dissolution rates vary considerably with pH; they are highest at acidic pH values and decrease with pH to pH 5.3. At pH values >5.3, the dissolution rate is nearly independent of pH. Under similar experimental conditions (i.e. far from equilibrium at circumneutral pH and room T and P), the dissolution rates determined by AFM are typically about an order of magnitude smaller than those determined by bulk powder experiments (Arvidson *et al*., 2003) and from calcium fluxes measured in the AFM fluid cell effluent solution (Duckworth and Martin, 2004). There are several reasons for the disagreement between the measured macroscopic and nanoscale dissolution rates, including the fact that AFM measurements are carried out on relatively smooth cleavage surfaces, which are less reactive than areas of crystal surfaces that have large steps or deep etch pits, the normalization of rates by inferred geometric areas and the use of mineral powders which are likely to expose highly reactive surfaces to the solution in bulk experiments (Dove and Platt, 1996; Arvidson *et al*., 2003; Lüttge *at al*., 2003; Lüttge, 2005).

Calcite growth from aqueous solution

Growth studies by AFM have increased our understanding of calcite growth kinetics and crystallization mechanisms significantly. Direct homogeneous precipitation from solution requires a certain critical value of supersaturation; below this value there is a region in which growth is only possible if there is an existing seed crystal as a substrate. This metastable regime is commonly investigated by AFM in crystal growth experiments. Direct observations of nanoscale growth and its dependence on the chemical and physical characteristics of the solution has helped confirm existing growth models, which were based on the determination of growth rates from changes in bulk solution composition with time. In addition, AFM observations have shown the limitations of these models and have suggested theoretical modifications (e.g. Rashkovich *et al*., 2006).

Classical crystal-growth theory relates growth kinetics to the degree of supersaturation. However, the solution composition may also affect the growth kinetics of calcite via the pH (Ruiz-Agudo *et al*, 2010*b*), Ca^{2+} to CO_3^{2-} concentration ratio (Nehrke *et al*., 2007; Perdikouri *et al*., 2009; Larsen *et al*., 2010; Stack and Grantham, 2010), ionic strength (Zuddas and Mucci, 1998) or the presence of organic matter (Hoch *et al*., 2000). To develop predictive models that account for the influence of all of these parameters on the growth of calcite, their effects must be quantified in isolation. These effects cannot be calculated *a priori* and this is one of the areas that AFM experiments address by measuring step kinetics as a function of these parameters (Qiu and Orme, 2008). Furthermore, because growth (and dissolution) kinetics are affected not only by the chemical and physical parameters of the solution but also by the surface microtopography (Jordan and Rammensee, 1998), nanoscale investigations are critical to the establishment of accurate kinetic models.

Mechanisms and kinetics of calcite growth: control of the saturation state.

Direct observations using AFM have confirmed that calcite growth takes place by the spreading of pre-existing steps, the advancement of layers that are one unit cell high from surface defects (Hillner *et al*., 1992; Gratz *et al*., 1993) or by two-dimensional surface nucleation (Dove and Hochella, 1993) (Fig. 4). The first AFM studies of the mechanisms and kinetics of calcite growth as a function of supersaturation were published in 1993. These studies reported contradictory observations regarding calcite growth mechanisms and their relation to solution supersaturation. Gratz *et al*. (1993) concluded that growth was controlled by attachment of growth units at steps rather than at terraces, and that surface diffusion

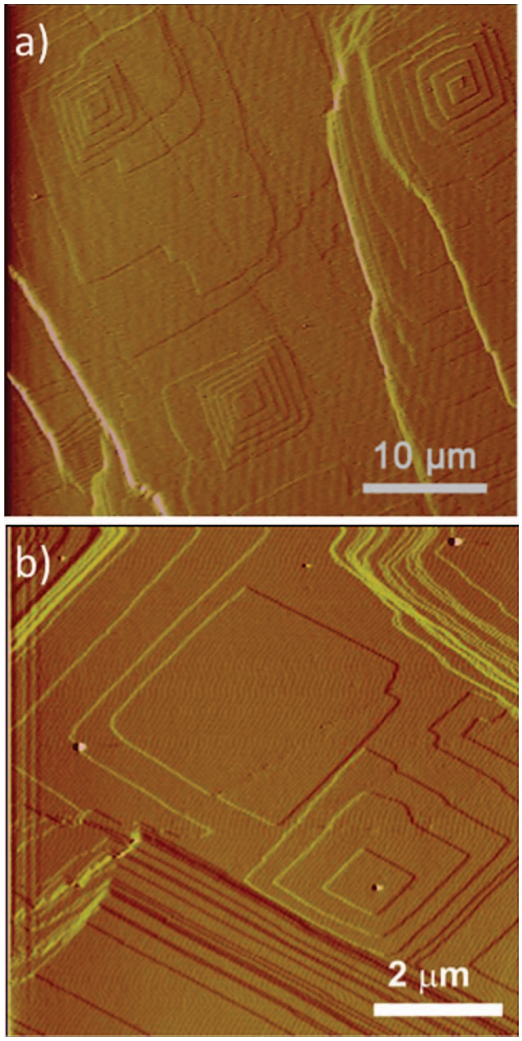

FIG. 4. Growth mechanisms on calcite {10$\bar{1}$4} surfaces as seen by AFM: (*a*) spiral growth; and (*b*) two-dimensional nucleation.

of the building units was limited in the case of calcite. The step source was uniquely growth spirals, and two-dimensional nucleation was not observed even at high supersaturation (e.g. $\Omega = 6.9$). In agreement with these observations, Hillner *et al*. (1993) found that the main growth mechanism of calcite cleavage faces was the propagation of layers that are one unit cell high and emerge from growth spirals with an effective rotation frequency (i.e. the product of the step velocity and step density as an indicator of linear growth rate) depending linearly on supersaturation. Dove and Hochella (1993) also observed such a linear dependence, and they concluded that surface diffusion was not an issue during calcite growth. They found that two-dimensional nucleation became an increasingly important growth mechanism at much lower supersaturation values than those found by Gratz *et al*. (1993) and Hillner *et al*. (1993). More recently, it has been shown that, close to the equilibrium, the acute and obtuse step velocities do not show a linear dependence on supersaturation as predicted by classical crystal growth theory (Teng *et al*., 1999) (Fig. 3*b*). The superlinear dependence of calcite step-spreading rates on supersaturation indicates that the step velocity is limited not only by the rate of kink motion along steps (assumed to vary linearly with supersaturation) but also by their generation rate (Teng *et al*., 1999; Rashkovich *et al*., 2006). Thus, the observed dependence of step-spreading rates on supersaturation suggests an increase in kink density with supersaturation. The direction-specific kinetic behaviour observed in calcite is explained by Teng *et al*. (1999) by considering differences in steric restrictions for solution incorporation between obtuse and acute steps. However, as discussed below, differences in the hydration of non-equivalent steps may well explain this observation.

Teng *et al*. (2000) showed that the crystal growth mechanism in calcite depends on the distance from equilibrium. Close to equilibrium, growth takes place by the advancement of steps emerging from surface defects, including screw dislocations. Once a threshold supersaturation is exceeded, two-dimensional nucleation becomes an increasingly important source of growth steps. This study also showed that the dependence of growth rate on the degree of saturation of the solution is ultimately controlled by the structure of the step source (i.e. simple single source spiral, multiple single source spiral or two-dimensional nuclei). Macroscopic growth rates determined from bulk measurements are the sum of the contributions of the different crystal faces and surface structures, each of them having a characteristic reactivity, and therefore, care must be taken when inferring growth mechanisms from the temporal evolution of bulk-solution chemistry. Direct observation of the growing mineral surfaces thus seems critical for determining representative growth mechanisms and obtaining accurate rate laws.

Dependence of calcite growth kinetics on pH and temperature: thermodynamic vs. kinetic effects.

Most macroscopic or nanoscale calcite growth studies have been conducted at a constant pH varying from ~8 to 10, or by varying the degree of supersaturation with respect to calcite and the $a\mathrm{Ca}^{2+}/a\mathrm{CO}_3^{2-}$ ratio together with the pH. This hinders an unequivocal evaluation of the effect of pH on calcite growth kinetics. In addition, the majority of AFM growth studies are carried out at room temperature. Calcite solubility decreases with increasing temperature, and therefore it is to be expected that an increase in temperature (for a constant solution composition) will result in an increase in growth rate. On the other hand, changes in the pH of the precipitating fluid result in the modification of the solution speciation, and therefore of its degree of supersaturation, also affecting calcite growth kinetics. Apart from these thermodynamic effects, several AFM studies have reported purely kinetic effects on calcite growth with changing pH or temperature. Wasylenski *et al*. (2005*a*) found that step advancement rates are greater at higher temperatures (for a constant driving force). This is not a thermodynamic effect as the decrease in solubility of calcite with increasing temperature is taken into account by using a different value for the solubility product. At higher temperatures, the growth rate is more sensitive to changes in supersaturation. Ruiz-Agudo *et al*. (2011*a*) showed that at fixed supersaturation and ion activity ratio, pH-sensitive changes in surface speciation and the effect of OH^- ions on solute hydration may also affect calcite growth. Furthermore, changes in two-dimensional island morphology observed at high pH are ascribed to the stabilization of polar scalenohedral faces by the presence of OH^- ions. According to the mechanistic model for the kinetics of carbonate crystal growth (Sternbeck, 1997; Nilsson and Sternbeck, 1999), these authors suggested that calcite growth occurs mainly by CaCO_3^0 incorporation at $>\mathrm{CaHCO}_3^0$ surface sites. This species should be more easily incorporated than free Ca^{2+} ions due to the faster exchange rates in the ion hydration shells when $\mathrm{H_2O}$ molecules are substituted by other ligands. However, at pH above 9, Ca^{2+} incorporation at $>\mathrm{CaHCO}_3^0$ sites also contributes to calcite growth as a result of changes in Ca^{2+} hydration induced by the presence of the strongly hydrated OH^- group. A similar effect could also explain the results of Wasylenski *et al*. (2005*a*) described above, as temperature modifies the dynamics of $\mathrm{H_2O}$ exchange between an ion solvation shell and its surrounding medium (Kowacz and Putnis, 2008).

Differential sensitivity of non-equivalent step propagation to solution stoichiometry

Natural ocean and continental waters supersaturated with respect to calcite are generally characterized by Ca^{2+} to CO_3^{2-} concentration ratios different from unity (Larsen *et al*., 2010 and references therein). Macroscopic and microscopic growth studies of different binary non-Kossel crystals have shown the significant influence of the solution ion-activity ratio on both growth rate and morphology (Larsen *et al*., 2010 and references therein). In the case of calcite, although Gratz and coworkers had reported that the velocity anisotropy of macrosteps changed with the Ca^{2+} to CO_3^{2-} ratio in solution in 1993, it is only recently that the effect of solution stoichiometry on calcite growth has been studied systematically (Nehrke *et al*., 2007; Perdikouri *et al*., 2009; Larsen *et al*., 2010; Stack and Grantham, 2010). Atomic force microscopy has revealed interesting insights into the atomic-scale mechanisms underlying the effect of solution stoichiometry on calcite growth. Perdikouri *et al*. (2009) found that, for a given supersaturation, the maximum calcite growth rate (expressed as v_{sum}) occurs in a non-stoichiometric solution with a calcium/carbonate activity ratio close to 2, and that the growth rate decreases asymmetrically around this value. These observations suggest that (1) calcium ions have lower integration frequencies to kink sites at the calcite surface during growth than carbonate ions, and (2) cation attachment is the rate-limiting process for calcite growth [as was previously inferred from experimental and computational studies in the case of baryte by Piana *et al*. (2006)], probably due to the fact that calcium ions dehydrate at slower rates than carbonate ions. This is at variance with the theoretical models describing the dependence of the step velocity on solution stoichiometry for binary ionic crystals that assume equal attachment and detachment frequencies of the lattice ions (Zhang and Nancollas, 1998; Rashkovich *et al*., 2006). Perdikouri *et al*. (2009) also observed changes in the morphology of growth features with

varying solution stoichiometry in their AFM experiments.

Recent studies by Larsen *et al*. (2010) and Stack and Grantham (2010) have shown that the velocities of acute and obtuse step spreading have different sensitivities to solute activity ratios in solution, reaching maximum values at $a\mathrm{Ca}^{2+}/a\mathrm{CO}_3^{2-} < 1$ and $a\mathrm{Ca}^{2+}/a\mathrm{CO}_3^{2-} \geqslant 1$ for acute and obtuse steps, respectively. Thus, a higher relative activity of CO_3^{2-} ions is required to accelerate the growth of acute steps compared to obtuse steps, indicating that cation dehydration is not the only parameter controlling the kinetics of step advancement. This anisotropy in obtuse and acute step kinetics could be due to differences in step hydration and the processes controlling the kinetics of step advancement, i.e. kink formation and spreading (Ruiz-Agudo *et al*., 2011*b*). The kinetics of crystal growth is ultimately determined by the frequency of attachment of building units at kink sites on the crystal surface. Sparingly soluble minerals typically have low kink-site densities, so that kink nucleation is the main process controlling the kinetics of step propagation (De Yoreo *et al*., 2009). Density functional theory calculations have suggested that H_2O binds more strongly to acute steps (Lardge *et al*., 2010) and therefore, the presence of hydration H_2O in this case could present a stronger resistance toward ion diffusion to the crystal surface and would have a stronger impact on kink formation at acute steps relative to obtuse steps. Thus, kink nucleation could be diffusion-limited on acute steps. This is supported by atomistic simulations that indicate that the creation of a kink site by attaching a building unit at a step edge requires four times more energy for acute steps than for obtuse steps (de Leeuw *et al*., 2001). Cation attachment to the surface may be assisted by the presence of adsorbed carbonate ions, as is the case for sulfate ions with baryte (Piana *et al*., 2006), thus facilitating kink nucleation and increasing the rate of advancement of acute steps relative to obtuse steps. This may explain why the maximum spreading rate of calcite acute steps at fixed supersaturation occurs at $a\mathrm{Ca}^{2+}/a\mathrm{CO}_3^{2-} < 1$ (Larsen *et al*., 2010; Stack and Grantham, 2010). Unfortunately, the validity of this idea cannot be unequivocally established experimentally, although molecular dynamic simulations may shed more light on the origin of the different sensitivities of acute and obtuse step spreading rates to building-unit activity ratios in solution.

The origin of reversed geometries of calcite growth hillocks.

Calcite can show specific morphologies when growing at very slow rates, under close-to-equilibrium conditions (Teng *et al*., 1999). This macroscopic observation reflects a nanoscale phenomenon associated with differences between the relative rates of step advancement along specific crystallographic directions that results when the supersaturation and other solution characteristics (such as the solution stoichiometry or composition of background electrolytes) are modified. In normal circumstances, growth perpendicular to the crystallographic directions $[\bar{4}41]_+$ and $[48\bar{1}]_+$ (i.e. obtuse steps) is faster than growth perpendicular to the $[\bar{4}41]_-$ and $[48\bar{1}]_-$ acute steps. A change in the relative rates of step spreading (i.e. $v_- > v_+$) results in the formation of *reversed* morphologies including calcite growth hillocks (Fig. 5). This was first reported by Teng *et al*. (1999) in crystals growing in solutions containing NaCl at $a\mathrm{Ca}^{2+}/a\mathrm{CO}_3^{2-} = 1$ in near-equilibrium conditions (i.e. low supersaturation). It has been observed recently at low $a\mathrm{Ca}^{2+}/a\mathrm{CO}_3^{2-}$ ratios (Larsen *et al*., 2010) and in the presence of specific background electrolytes such as KCl and CsCl (Ruiz-Agudo *et al*., 2011*b*). Teng *et al*. (1999) claimed that the growth-modifying effects of impurities (Mg, Sr or Ba) produced these morphologies. However, because the impurity ions have distinct preferences for acute (Mg^{2+}) or obtuse (Sr^{2+}, Ba^{2+}) steps (Paquette and Reeder, 1995; Reeder, 1996; Davis *et al*., 2004), pinning and reduction of both acute or obtuse step spreading rate should occur. Therefore, it seems unlikely that impurity pinning causes these reversed geometries.

As described above, obtuse step advancement may be controlled mainly by the availability of calcium in solution for its attachment to a kink site, whereas acute step advancement may be governed by kink-site nucleation and ultimately by the hydration of carbonate at the surface (Ruiz-Agudo *et al*., 2011*b*). Therefore, either decreased hydration of carbonate surface sites in the presence of background electrolytes such as KCl and CsCl, or carbonate-assisted attachment of calcium to growth sites at low $a\mathrm{Ca}^{2+}/a\mathrm{CO}_3^{2-}$ could accelerate kink nucleation at acute steps and thus increase the velocity of propagation of such steps relative to obtuse steps. In this model, the obtuse-step propagation rate may be more sensitive to the reduction in the activity of

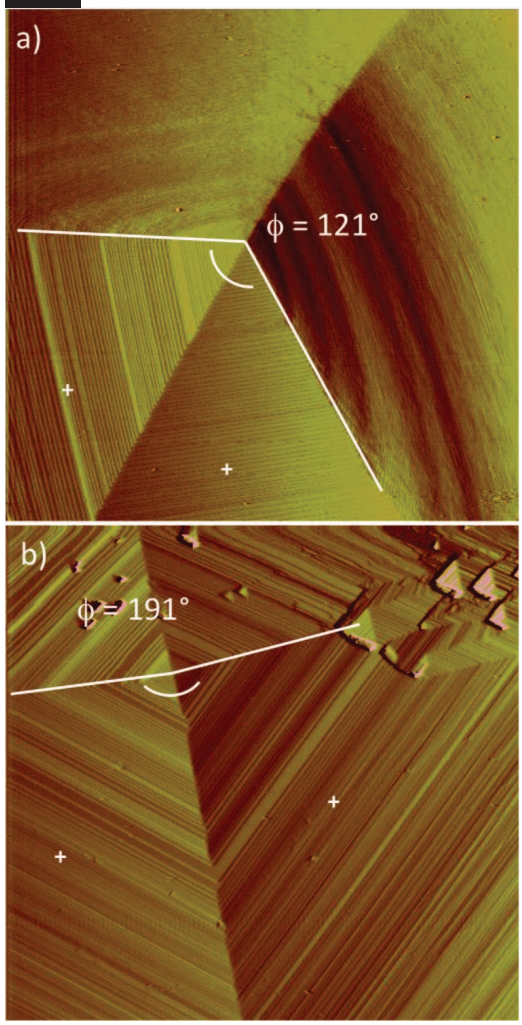

FIG. 5. Development of reverse morphologies in spiral hillocks: (*a*) growth hillock formed during growth in NaCl-bearing solutions; and (*b*) the same spiral in (*a*) after changing the background electrolyte of the growth solution to CsCl. Images are 10 μm × 10 μm.

calcium in solution than the acute-step propagation rate. This would explain the change in the relative rate of step spreading detected at low supersaturation (Teng *et al*., 1999). Regardless of the validity of this model, these observations show the sensitivity of the direction-specific reactivity of calcite surfaces to differences in solution chemistry and suggest different ways in which living organisms might modulate the morphology or properties of biogenic carbonates through slight changes in the chemistry of the precipitating fluid.

Effect of inorganic additives on calcite growth and dissolution

The influence of impurities or additives on calcite growth and dissolution has attracted much research attention due to the widespread occurrence of calcite in Earth environments and the geochemical and environmental importance of these processes. Additives (i.e. ions or molecules that are different from the constituents of the solvent and crystal), which vary in complexity from small ions such as magnesium to large polysaccharides and proteins, can interact with mineral surfaces in ways that result in their incorporation into the crystal, the pinning of steps, modifications of the energetics of the surface, and changes in the kinetics of growth and dissolution (Qiu and Orme, 2008). Macroscopic growth and dissolution studies rely on the study of the calcite crystal structure and the subsequent changes in crystal morphology induced by additives to infer the mechanisms of such interactions. However, the use of scanning probe microscopy techniques including AFM, enables *in situ* measurements and observations in real time, increasing our understanding of the interaction mechanisms of additives with calcite during dissolution and growth. These observations allow measurement of step advancement rates, terrace widths and defect structures, providing kinetic and thermodynamic data that reflects additive–crystal interaction at the crystal surface during growth or dissolution. Moreover, AFM images of the crystal surface provide details and specific information about the terraces, ledges and kinks influenced by additives that are adsorbed or incorporated along specific crystallographic directions (Wang *et al*., 2011).

Kinetic effects of 'inert' background electrolytes on calcite growth and dissolution

Water in contact with rock-forming minerals contains significant amounts of inorganic ions in solution. The effect of these background inorganic electrolytes or the ionic strength (IS) effect (Buhmann and Dreybrodt, 1987) on mineral growth and dissolution kinetics has been traditionally ascribed to changes in solubility. The strong long-range electric fields emanating from the ions of the background electrolyte reduce the

activity of the ions building the crystal due to charge screening and therefore reduce supersaturation. Therefore, on a purely thermodynamic basis, the dissolution rates of minerals in the presence of electrolytes should increase due to an increasing driving force and the growth rates should decrease due to a decreasing driving force. Monovalent NaCl and KCl are commonly used in mineral dissolution or growth experiments as background electrolytes to fix the ionic strength of solutions. The ions in these electrolytes are generally regarded as 'inert' (i.e. they are not adsorbed on or incorporated in the growing mineral surface or they may do so to a very limited extent) and thus changes of a specified variable (e.g. dissolution rate) as a function of ionic strength are typically measured using these salts as background electrolytes. Relatively few studies have systematically examined the effect of ionic strength on calcite growth and dissolution, and there are even fewer studies that have used AFM or other SPM techniques.

Some recent AFM studies have found significant differences in the dissolution and growth rates of carbonate (calcite and dolomite) and sulfate (baryte) minerals in solutions containing different electrolytes at similar ionic strengths (Kowacz and Putnis, 2008; Ruiz-Agudo *et al*., 2009, 2010*b*, 2011*b*). These findings suggest that the ionic strength effect is species dependent. They also show that ions with high or low surface charge densities produce different effects on mineral dissolution and growth, which cannot be explained by continuum electrostatic models such as Debye–Hückel (i.e. those considering the ions as point charges) (Collins, 1997). As discussed above, experimental and computational studies have shown that the crystal growth and dissolution kinetics of sulfate and carbonate minerals are controlled by cation hydration–dehydration dynamics (Pokrovsky and Schott, 2002; Piana *et al*., 2006). Thus, any factor affecting cation solvation should alter growth and dissolution rates. The degree of solvation or hydration of a crystal-building cation, both at the mineral surface and in solution, is governed by the strength of ion–water and ion–ion interactions. The presence of electrolytes can modify these interactions. In dilute electrolyte solutions, ion–ion interactions dominate and the stabilization of H_2O molecules in the hydration shells of calcite-building units by the counter ions present in solution enhances the unfavourable entropic effect on calcite dissolution. The formation of ion pairs in solution reduces this effect, resulting in an inverse correlation between dissolution rates and background ion separation in solution (Kowacz and Putnis, 2008, and references therein). However, the hydration of crystal-constituting ions in electrolyte solutions of high ionic strength is influenced by the interaction between background ions and water molecules. The main differences in calcite dissolution kinetics under these conditions are observed for different background anions as they control the solvent structure around Ca^{2+} and therefore, calcium removal from the structure. In this case, dissolution rates correlate with the mobility of background ions and therefore with the volume of water affected by the presence of the background ions.

Effect of inorganic impurities on calcite growth: step pinning and impurity incorporation models

The process of ion incorporation into minerals is a key control on the reactivity and cycling of elements in biogeochemical systems and therefore, it is critical in explaining and predicting numerous ocean and Earth surface processes. In particular, ions incorporated in biogenic marine carbonates are widely used as proxies for changes in ocean chemistry and palaeoclimate. These proxies increase our understanding of past climate and how it evolves with time, thus enhancing our ability to predict future climate change. If Mg, Sr or Ba are going to be used as reliable proxies for the growth conditions of biogenic carbonates, detailed knowledge of the underlying mechanism of element partitioning at ambient temperatures is essential. The partitioning can be overprinted or influenced by phenomena unrelated to climate change. This has motivated significant research on the incorporation of foreign ions, mostly divalent cations, into carbonate minerals and their effect on mineral growth. Recent AFM studies have also dealt with the incorporation of monovalent cations such lithium and sodium on calcite growth. Lithium in particular, has a significant influence on calcite growth (Ruiz-Agudo *et al*., 2009, 2011*b*; Wang *et al*., 2011).

This is a very complex topic whose theoretical treatment uses two main approaches: (1) the *step-pinning model* (Cabrera and Vermilyea, 1958; Kubota and Mullin, 1995; van Enckevort *et al*., 1996; De Yoreo and Vekilov, 2003); and (2) the *impurity-incorporation model* (e.g. Davis *et al*., 2000; De Yoreo and Vekilov, 2003). The major

difference between the two models is that in the step-pinning model, the adsorption of impurities is a reversible process, whereas in the impurity-incorporation model the impurities in the crystal structure cannot be released back to the solution easily. The classical impurity models were developed and tested using bulk measurements and experiments, but macroscopic experiments do not provide detailed information about step dynamics during crystal growth. A complete picture of the processes occurring at the mineral–solution interface requires techniques that allow nanoscale observations such as AFM (Astilleros *et al*., 2010). In particular, kinetic data obtained in AFM studies showing step advancement rates as a function of solution supersaturation for different impurity concentrations in the growing fluid are commonly used to infer the mechanism of crystal−impurity interactions (Astilleros *et al*., 2010; Davis *et al*. 2000) (Fig. 6).

The *impurity-incorporation model* assumes that the impurities incorporated into the calcite structure form a solid solution. It is then considered that a solid with this composition is more soluble than pure calcite, as the incorporation of the impurity ions destabilize the crystal lattice and consequently increase its solubility (Davis *et al*., 2004), so that the supersaturation of the aqueous solution with respect to a surface layer of this solid solution will be lower (e.g. Stephenson *et al*., 2008). As a result, the step velocity in the presence of the impurity will always be lower than in the pure system. The typical example of an ion that is considered to follow this model during its interaction with calcite is magnesium. Magnesium is the most abundant of the minor elements that are commonly incorporated in calcite and displays some of the strongest correlations with growth conditions, mainly temperature but also salinity and seawater Mg/Ca ratios (Wasylenski *et al*., 2005*a*). There is general agreement that the presence of magnesium in an aqueous solution has a strong inhibiting effect on the growth of calcite due to the its effect on the thermodynamics of the system, as described above (Davis *et al*., 2000, 2004; Dove *et al*., 2004; Wasylenki *et al*., 2005*a*; Stephenson *et al*., 2008; Astilleros *et al*., 2010). Studies have also shown that magnesium has a strong preference for acute steps if surface reactivity is the growth-limiting factor, as shown by morphological changes in growth features in the presence of this ion. However, when calcite growth is controlled by mass transport, magnesium tends to preferentially incorporate at obtuse steps (Wasylenki *et al*., 2005*a*). Other ions such as Mn^{2+} (Astilleros *et al*., 2002) and SO_4^{2-} (Vavouraki *et al*., 2008) also seem to interact with calcite following the impurity-incorporation model.

The *step-pinning model* assumes that impurity adsorption at kink sites on step edges causes the pinning of the steps as monolayers on the surface, hindering step advancement. In this model, if the impurity concentration is high enough, steps fail to advance and no growth occurs (producing a dead zone). Impurity adsorption is a reversible process in this model and when a threshold supersaturation is reached, adsorbed impurities are removed from the mineral surface, and growth steps rapidly achieve the velocity characteristic of the pure solid at that supersaturation. Several authors have suggested that the step-pinning model provides a better description of the effect of cations such as Sr^{2+} or Ba^{2+} and anions such as PO_4^{3-} on calcite growth (Dove and Hochella, 1993; Astilleros *et al*., 2000; Wasylenski *et al*., 2005*b*). This model is reflected in step-rate data obtained by AFM as an increase in step velocity at a certain threshold solution supersaturation that approaches the value of the pure system.

Astilleros and coworkers (Astilleros *et al*., 2003, 2010; Freij *et al*., 2004) have shown that classical impurity models are unable to account for the nanoscale growth behaviour of calcite in the presence of certain ions as seen by AFM. These models are unable to explain two of their observations: (1) the rate of step advancement is variable, depending on the layer considered (for a given supersaturation and impurity concentration); and (2) growth inhibition of the first layer by foreign cations is not always detected. This has been found for cations including Mg^{2+}, Sr^{2+} and Mn^{2+} (Astilleros *et al*., 2003, 2010; Freij *et al*., 2004) (Fig. 7). A critical point of their discussion is the argument that an increase in the solubility of the solid phase due to the incorporation of foreign ions does not necessarily result in a decrease of the effective supersaturation of the growth solution, contrary to the principles of impurity-incorporation models. It has to be considered that in the modelling of systems with an impure solid in contact with an aqueous solution, the supersaturation cannot be expressed by a single value, as it is a function of the solid and the aqueous phase compositions. An aqueous solution can be undersaturated with respect to a pure phase and supersaturated with respect to a more soluble solid solution. The general thermo-

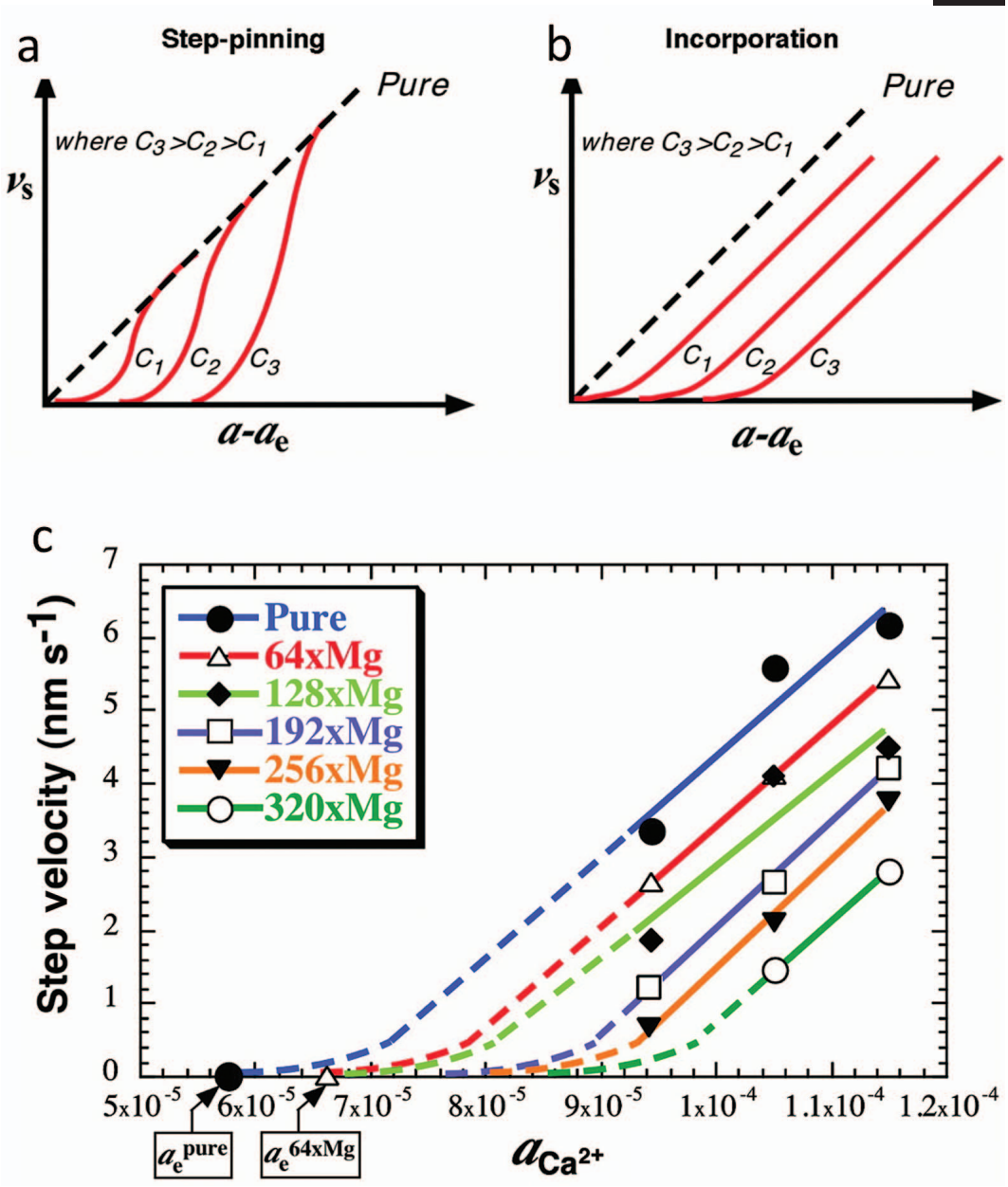

FIG. 6. Theoretical plots illustrating the dependence of step velocity (v_s) on supersaturation ($a-a_e$) for (*a*) step pinning and (*b*) impurity-incorporation models; C_i is the impurity concentration in solution. (*c*) Dependence of step velocity determined by *in situ* AFM experiments on calcium activity ($a\mathrm{Ca}^{2+}$) as a function of Mg^{2+} concentration for the $[\bar{4}41]_-$ and $[48\bar{1}]_-$ step directions. Comparison of this plot with the theoretical plots shown in (*a*) and (*b*) suggests that Mg^{2+} inhibits calcite growth via an incorporation mechanism. From Davis *et al*. (2000) reprinted with permission from AAAS.

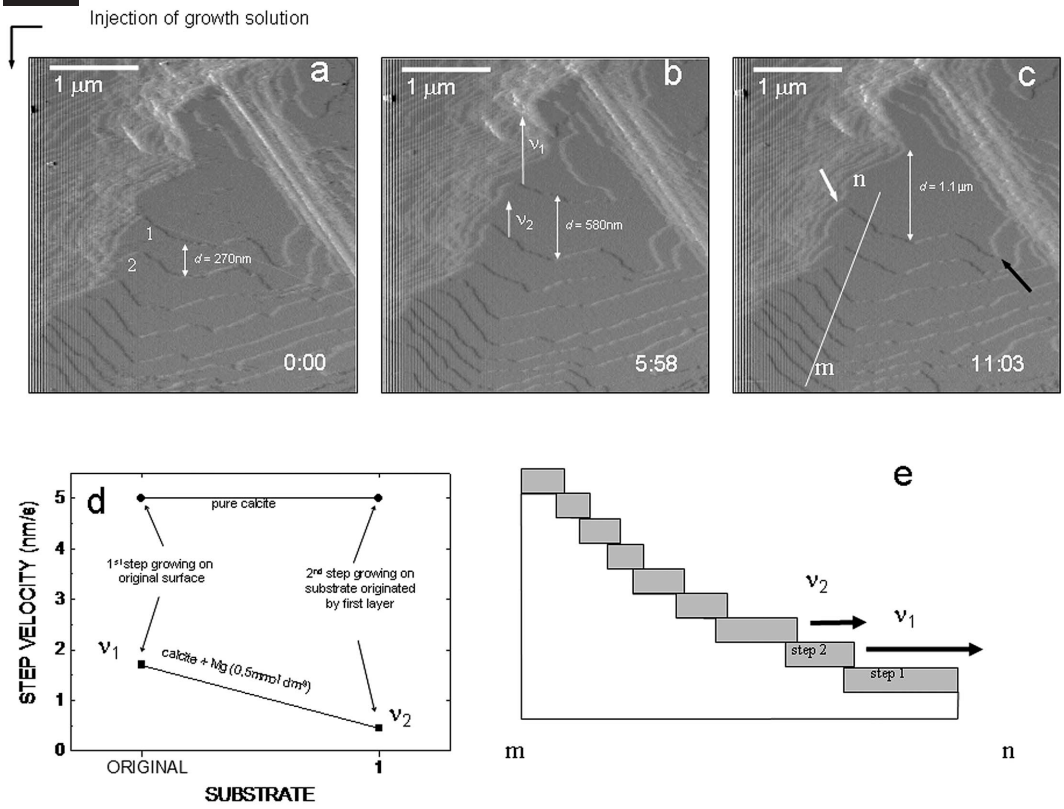

FIG. 7. (*a*–*c*) Growth sequence of a calcite {10$\bar{1}$4} surface in the presence of Mg, showing the control of the surface on the growth process. The whole sequence of AFM images (deflection images) took ~11 min. (*d*) The measured step velocities for <$\bar{4}$41>$_+$ on different substrates generated during growth, clearly show the inhibiting role of the newly formed substrate on the step advancement. The topographic cross section (*e*) shows the relationship between original and newly formed layers. Reprinted from Astilleros *et al*. (2010) with permission from Elsevier.

dynamic principles governing solid-solution–aqueous-solution (SS–AS) systems on which this assertion is made are well established (Glynn and Reardon, 1990; Tesoriero and Pankow, 1996) and have recently been reviewed by Prieto (2009). This argument is applicable to all SS–AS systems, independent of their thermodynamic properties.

In an AFM study of the role of Mg in the growth of calcite by Astilleros *et al*. (2010), the variable rates of step advancement of successive growth layers are explained by postulating that the substituting cations are randomly distributed in the first growth layer, but that cation distribution in successive layers is controlled by the structure of the layers beneath. The retardation in step advancement is caused by the relaxation of the strain normal to the first growth layer, which is highly disordered and strained as a consequence of the differences in size and thus bond lengths of the substituted cations. The studies by Astilleros *et al*. (2010) emphasize the importance of detailed *in situ* nanoscale and microscale observations in understanding impurity-specific interactions with calcite growth surfaces, a task for which AFM is an appropriate and important tool.

Influence of foreign inorganic ions on calcite dissolution: site-specific and non-specific effects.

Foreign ions affect mineral growth and they can also have a significant impact on dissolution (Fig. 8). It is generally accepted that these effects are the result of the direction-specific adsorption of ions at calcite surface sites, which can be

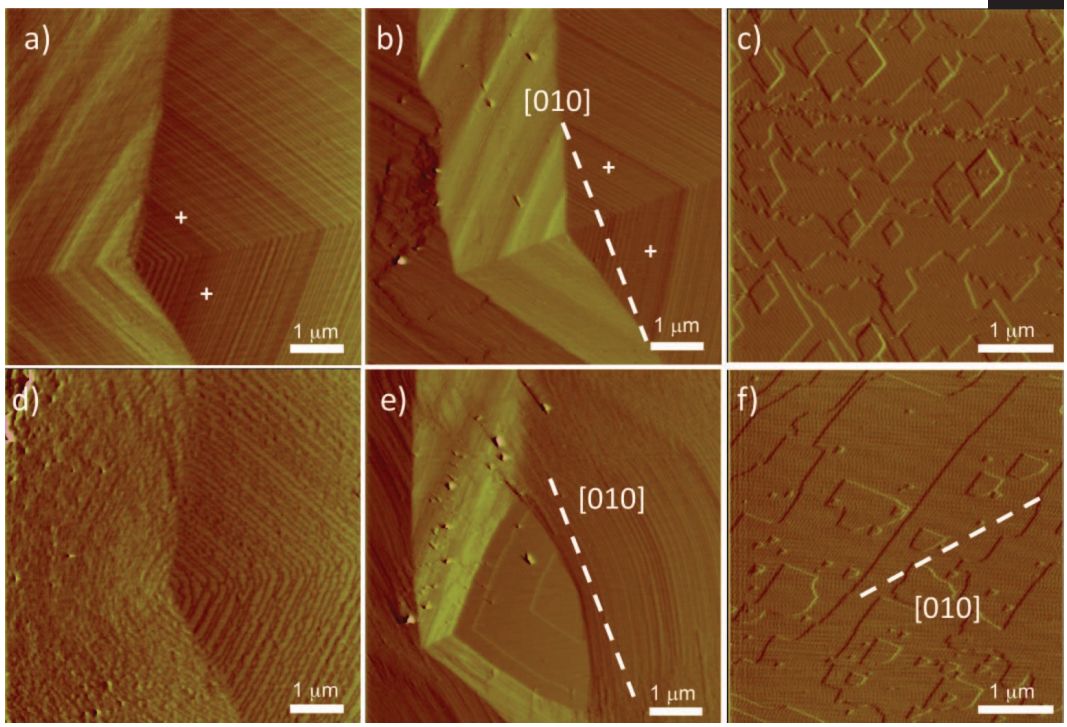

FIG. 8. Changes in the morphology of (*a*,*b*,*d*,*e*) growth and (*c*,*f*) dissolution features induced by the presence of additives. (*a*,*b*) Growth spirals; and (*c*) etch pits formed in pure solutions. (*d*) The same features in (*a*,*b*,*c*) after adding L-aspartic acid; and (*e*,*f*) Li^+ to the solution.

considered as reversible or essentially irreversible, depending on the residence time of the impurity ion at the surface sites relative to that of calcium. Adsorbed impurities pin steps at specific points, leading in the case of calcite to variations in rates of step retreat and etch-pit density, modifications in the anisotropy of step velocities, and changes in the rhombohedral morphology of etch pits on cleavage surfaces (Lea *et al*., 2001; Freij *et al*., 2005; Vinson and Luttge, 2005; Arvidson *et al*., 2006; Teng *et al*., 2006; Harstad and Stipp, 2007; Perez-Garrido *et al*., 2007). Furthermore, dissolution processes can also be affected by divalent cations, present as trace elements in solid solution in calcite at ppb or ppm levels. It has been observed that if the original calcite substrate has high trace-cation concentrations (particularly Mn), the obtuse step-advancement rate during dissolution is systematically reduced (Harstad and Stipp, 2007). In addition, etch pits develop a nearly triangular shape, as a result of the blocking of obtuse−obtuse corners. This is thought to be due to the release of trace cations during dissolution and their re-adsorption at active surface sites (step edges and corners) (Harstad and Stipp, 2007).

The influence of impurities on calcite dissolution has received much less attention than their influence on crystal growth and has been limited mostly to the effect of divalent cations (see above). The influence of magnesium on calcite dissolution (due to its environmental significance) has been the subject of several nanoscale and microscale studies using AFM and other techniques including vertical scanning interferometry (VSI) (e.g. Arvidson *et al*., 2006; Ruiz-Agudo *et al*., 2009; Xu and Higgins, 2011). At concentrations <1 mM and in conditions that are far from equilibrium, Mg^{2+} inhibits calcite dissolution by reducing the etch-pit spreading rate (Arvidson *et al*., 2006). This effect seems to be dependent on the saturation state of the solution. At low supersaturation, Mg^{2+} has a limited inhibitory effect on calcite dissolution at concentrations of

10^{-3} molal, but the inhibition of calcite dissolution by Mg^{2+} at this concentration is more significant closer to equilibrium (Xu and Higgins, 2011). Obtuse–obtuse rounding of calcite etch pits in the presence of Mg^{2+} has also been reported (Ruiz-Agudo *et al*., 2009). Other divalent cations including Mn^{2+}, Sr^{2+} and Zn^{2+} also act as dissolution inhibitors, and have shown a similar predilection for the obtuse–obtuse corner during calcite dissolution, as shown by the rounding of that corner in the presence of those ions (Lea *et al*., 2001; Freij *et a*l., 2005; Arvidson *et al*., 2006; Vinson *et al*., 2007). Interestingly, the inhibitory effect of impurities such as Mg^{2+}, Mn^{2+} and Sr^{2+} on calcite dissolution is strongly dependent on the presence of dissolved carbon-bearing species (Lea *et al*., 2001; Vinson and Luttge, 2005; Arvidson *et al*., 2006; Vinson *et al*., 2007). This, together with the above described effects that indicate that ions preferentially incorporate in +/+ steps regardless of their ionic radius, seems to indicate that these ions adsorb as $MeCO_3^0$ (where *Me* = Mg^{2+}, Mn^{2+} and Sr^{2+}), possibly through surface reaction with $>CaOH_2^+$ sites (Arvidson *et al*. 2006; Ruiz-Agudo *et al*., 2009). This large species would tend to be adsorbed at the more open obtuse steps.

As well as the effect of geologically relevant cations on calcite dissolution, the impact of heavy metals has attracted much attention due to the proven effectiveness of methods that involve water–carbonate surface interaction for the remediation of contaminated waters. The adsorption or incorporation of toxic heavy metals by calcite strongly reduces their bioavailability and avoids their assimilation by living organisms. Combined AFM and X-ray photoelectron spectroscopy (XPS) studies have shown that Ni^{2+} is adsorbed to a significant extent on calcite surfaces during dissolution (Hoffmann and Stipp, 2001). Hay *et al*. (2003) and Perez-Garrido *et al*. (2009) showed that Cd^{2+} has an inhibitory effect on calcite dissolution. There is a threshold concentration (0.005 mM), below which calcite dissolves at a similar rate to that in pure deionized water, and a regime at higher Cd^{2+} concentrations where dissolution is significantly affected. The presence of cadmium clearly affects the morphology of the etch pits formed during calcite dissolution; they alter from the typical rhombohedral shapes to an elongated pseudo-elliptical morphology. The spreading of these etch pits is clearly anisotropic, moving faster along the $[42\bar{1}1]$ direction than along the [010] direction. A similar anisotropy in etch-pit widening is also observed in dissolution in the presence of Hg^{2+}, the etch pits being triangular in morphology in this case (Godelitsas *et al*., 2003). *In situ* AFM calcite dissolution experiments in the presence of cobalt have shown significant interactions with calcite surfaces during dissolution, this is explained by adsorption at acute kinks, resulting in a change in the morphology of the etch pits from their characteristic rhombohedral shape to a near-triangular morphology (Freij *et al*., 2004). At high concentrations of divalent cations, the precipitation of secondary phases, consisting of $(Ca,Me)CO_3$ solid solutions in many cases, has been commonly reported (Godelitsas *et al*., 2003; Lea *et al*., 2003; Chada *et al*., 2005; Cubillas and Higgings, 2009; Perez-Garrido *et al*., 2009). The inhibition of calcite dissolution by the formation of sparingly soluble precipitates at step edges has been observed for trivalent cations such as lanthanum (Kamiya *et al*., 2004). Finally, a few studies have explored the influence of anions on calcite dissolution. Vavouraki *et al*. (2010) and Ruiz-Agudo *et al*. (2010*b*) reported changes in dissolution morphology induced by F^- and SO_4^{2-} ions. These ions seem to accelerate the overall dissolution rate of calcite.

Recent AFM studies have shown that foreign ions exert other non-specific effects on mineral dissolution. For example, highly hydrated ions (such as F^- or Mg^{2+}) significantly increase the etch-pit nucleation density compared to pure water or solutions of weakly hydrated ions. This effect is thought to be related to a reduction in the energy barrier for etch-pit nucleation due to disruption of the surface hydration layer (Ruiz-Agudo *et al*., 2009, 2010*b*). As for growth, it has been proposed that changes in growth morphology may not be solely due to specific interactions between ions and mineral-surface charges (Kowacz and Putnis, 2008; Ruiz-Agudo *et al*., 2010*b*). The presence of background ions tends to stabilize H_2O groups in ion hydration shells and at crystal surfaces. Increasing ion hydration reduces both repulsive interactions between ions with the same charge and attractive interactions between ions with opposite charges (Kowacz and Putnis, 2008; Ruiz-Agudo *et al*., 2010*b*). Therefore, polar faces that are not stable when calcite dissolution occurs in pure solutions and thus are not reflected in the morphology of the dissolution features, will be stabilized, whereas non-polar faces should be less stable in the presence of background electrolytes. This has been shown for the case of calcite dissolution in

the presence of F^- and Li^+ (Ruiz-Agudo *et al*., 2010*b*), and for baryte dissolution (Kowacz and Putnis, 2008).

Organic molecules in calcite–water interactions

In biomineralization, the interplay between the organic components and minerals is the key to understanding how crystal growth is controlled (Henriksen *et al*., 2004). Biomineralization occurs in matrices that are rich in complex organic molecules such as polysaccharides and proteins, with compositions that are specific to each species (Stephenson *et al*., 2008 and references therein). In the last 15 years, a series of AFM studies have explored the atomic-scale dynamics of calcite growth and dissolution in the presence of a variety of these compounds. These macromolecules seem to actively control calcite growth mainly by modulating biomineral morphology (Fig. 9). It has been proposed that a combination of electrostatic, stereochemical and geometric recognition processes occur between organic molecules and step edges on calcite surfaces. These specific interactions between biomolecules and steps on mineral surfaces are thought to change the free energies of the steps and thus modify the atomic-scale morphology of calcite. The characteristic step patterns that result from such interactions are ultimately reflected in the macroscale modifications of calcite crystal morphology in comparison to the shapes observed in pure systems (De Yoreo and Dove, 2004).

Due to their relevance to biomineralization in coccoliths, polysaccharides have been the subject of several calcite growth and dissolution studies using AFM. Oligosaccharides and polysaccharides seem to interact with steps on calcite surfaces during growth and dissolution. In particular, polysaccharides associated with the coccolithophore species *Emiliania huxleyi* preferentially interact with acute step edges (Henriksen *et al*., 2004; Yang *et al*., 2008), distorting the rhombohedral shapes observed in surface features and inhibiting dissolution. This specificity makes them effective modulators of calcite morphology. Amino acids, peptides and proteins have been

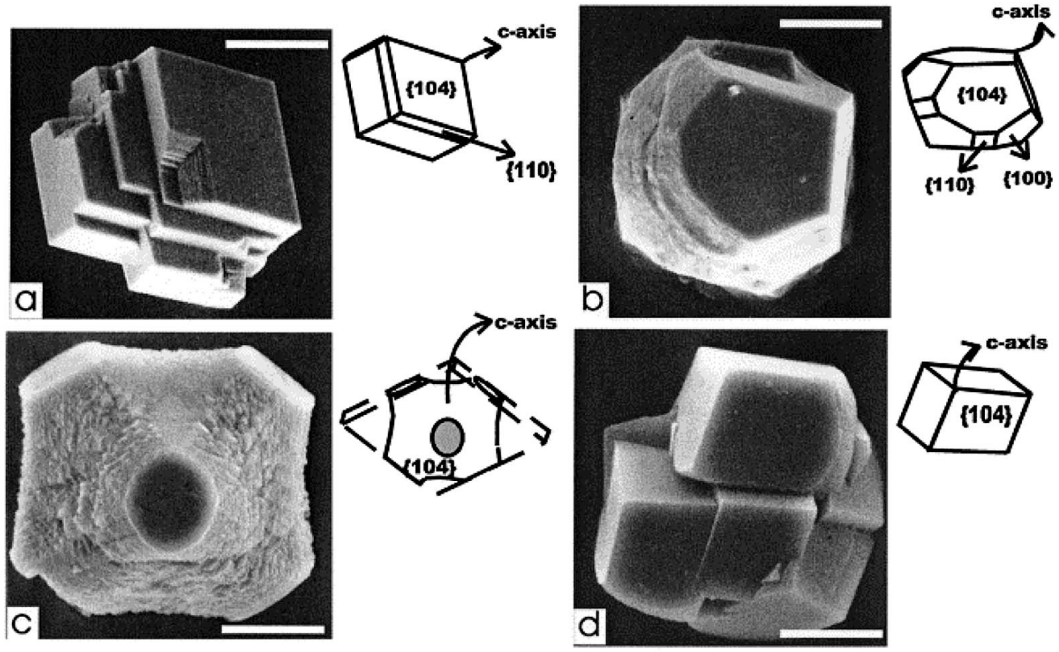

FIG. 9. Modulation of the rhombohedral calcite crystal habit by proteins. Scanning electron microscope images of calcite crystals grown in (*a*) 0.1 mg ml^{-1} (*b*) 10 mg ml^{-1} (*c*) 25 mg ml^{-1} and (*d*) 10 mg ml^{-1} lysozyme solutions. The crystals in (*a*–*c*) were collected after 50 h; the crystal in (*d*) was collected at the initial stages of growth. Scale bars are 20 μm. Reprinted from Jimenez-Lopez *et al*. (2003) with permission from Elsevier.

shown to play a major role as modulators of calcium carbonate biomineral growth, and consequently most of the research interest in this field has been concentrated on elucidating their mechanisms of interaction. For example, AFM studies on calcite growth and dissolution of proteins directly extracted from carbonate biominerals such as abalone nacre or oyster shell have shown that these proteins bind specifically to calcite steps (preferentially at acute steps), and at high enough concentrations are able to inhibit calcite growth in supersaturated solutions and prevent crystal dissolution in undersaturated solutions (Wierzbick *et al*., 1994; Walters *et al*., 1997; Treccani *et al*., 2006). However, low (nanomolar) concentrations of these peptides and proteins have been shown to increase the rates of step propagation during calcite growth (Eldhjad *et al*., 2006*a*,*b*).

As matrix proteins in biominerals include a high fraction (30–40%) of acidic amino acids, including aspartic acid and glutamic acid (Weiner, 1979), AFM growth and dissolution studies have also been done using these simpler amino acids and derived peptides with the aim of unravelling the complex mechanisms of protein–mineral interaction (e.g. Teng and Dove, 1997; Orme *et al*., 2001; Eldhjad *et al*., 2006*a*,*b*). It has been observed that these molecules induce morphological changes similar to those produced by more complex macromolecular assemblages. Furthermore, these studies have revealed interesting insights into the controls on both growth rates and mineral form during biomineralization processes. Unlike other impurities (see above), amino acid (aspartic acid) molecules, adsorbed on the calcite surface, do not seem to be incorporated into the bulk calcite, nor to pin step advancement during growth. According to AFM observations made by Orme *et al*. (2001), it has been suggested that these compounds alter calcite growth by modifying step-edge energetics. Studies using a series of poly-L-aspartates confirm the preferential binding of these compounds to calcite step edges, resulting in morphological changes. These effects are strongly chain length dependent, and a crossover in the step specificity is observed (from acute to obtuse) with increasing peptide chain length and the energy cost of surface dehydration, a step needed for peptide adsorption. It is then suggested that this process may be a plausible mechanism for the control of calcite morphology by small fluctuations in the primary structure of proteins (Eldhjah *et al*., 2006*b*). The growth enhancement observed in low-concentration peptide and protein solutions has been attributed to a reduction in the diffusive barrier for cation attachment caused by perturbations of the water of solvation at the calcite surface. This is supported by the fact that growth enhancement correlates with the relative hydrophilicity of peptides (Eldhjah *et al*., 2006*a*). Within the framework of this model, Stephenson *et al*. (2008) hypothesized that biomolecules assist the desolvation of strongly hydrated cations in the vicinity of the growing steps, as a possible mechanism to explain the fact that the presence of an aspartic-rich peptide increases Mg uptake by calcite during growth. In summary, these works suggest that biomolecules control calcite growth and trace metal uptake by facilitating the incorporation, desolvation and transport of ions to the calcite surface (Stephenson *et al*., 2008).

Recently, simple organic molecules including ethanol, methanol, maleic acid and phosphonates have been used in AFM studies of mineral growth and dissolution as analogues of more complicated macromolecules of relevance to biomineralization. It is considered that the effects of these simple analogues and proteins or polysaccharides on crystal growth kinetics have a similar origin at the atomic scale (Kowacz *et al*., 2007). These molecules are much simpler in principle to investigate, and can be used as analogues that facilitate the understanding of biomineralization processes. Kim *et al*. (2009) showed that specific poly(vinyl alcohol)s have a significant influence on calcite growth, mainly by inducing step roughening and macrostep formation. Growth in the presence of these molecules occurs by nucleation and growth of two-dimensional islands instead of by step flowing from surface defects, as a result of the additive adsorption on calcite surfaces that inhibits step spreading. This change in growth mechanism in the presence of adsorbed alcohol molecules is suggested by the authors as the strategy used by living organisms to create assemblies of microcrystals with occluded macromolecules. Atomic force microscopy experiments carried out in a 96% ethanol–water mixture have attempted to simulate biomineralization environments where water activity is assumed to be low and organic molecules are dominant. Ethanol binds strongly to calcite in these conditions, modifying its surface reactivity and representing a barrier for solute attachment and detachment, and as a consequence, for calcite growth and dissolution. This barrier is disrupted at

surface steps and defects, where preferential addition or removal of solutes may occur (Cooke *et al*., 2010; Sand *et al*., 2010). This is suggested as a potential mechanism by which living organisms control calcite growth and dissolution at preferred surface sites. Similar AFM studies on barite growth have shown that in dilute aqueous solutions of methanol, the kinetic barrier for barium approaching the crystal surface is reduced, leading to faster nucleation and accelerated step-growth velocity (Kowacz *et al*., 2007). Ruiz-Agudo *et al*. (2010*a*) observed changes in the morphology of dissolution features on calcite cleavage surfaces in the presence of HEDP, an organophosphonate compound. They also found that dissolution rates are drastically reduced at low phosphonate concentration, although they progressively increase with increasing concentration. The increased frequency of H_2O exchange in the hydration shell of calcium and the stabilization of polar steps by HEDP are suggested as mechanisms to explain the observed changes in morphology and dissolution kinetics. It can be inferred from these studies that changes in surface and solute hydration induced by organic molecules may control the effects of these compounds on calcite growth and dissolution. This conclusion supports the outcome of the studies by Elhadj *et al*. (2006*a*) and Stephenson *et al*. (2008).

Concluding remarks and future prospects

The invention and development of AFM has added an important experimental tool for mineralogists and crystallographers studying mineral–surface interactions *in situ* in real time. Atomic force microscopy has improved enormously our understanding of the dynamics of crystallization processes at the atomic scale. Furthermore, AFM has fuelled the current explosion of research into nanotechnology and has allowed mineralogists to explore new areas of mineral dissolution and growth, the way in which the composition of the solution can modify these mechanisms, and their kinetics. Crystal growth is a fundamental process in the origin of all rocks, and emphasis can now be focussed the process at an atomic scale. Calcite has been the subject of numerous AFM studies due to its relevance to many geochemical and biomineralization processes. In the last two decades, these studies have shown the ordered structure of the calcite surface and have provided direct evidence of the existence of H_2O bound to calcite surfaces. Furthermore, measurement of calcite growth and dissolution rates, terrace widths and defect structures, in pure solutions and in the presence of additives, have provided kinetic and mechanistic information on growth and dissolution processes that allows existing models derived from macroscopic experiments to be tested. This information has helped to clarify many aspects of crystal growth including: (1) the control exerted by the saturation state on the mechanism of calcite growth and dissolution; (2) the role of organic molecules in modulating calcite growth during biomineralization processes; and (3) the origin at a molecular scale of the effects of background electrolytes on calcite–fluid interactions.

The interpretation of molecular-scale observations such as those described in this review will increasingly depend on computational simulations of interactions between ions and water molecules at the fluid–solid interface. In turn, AFM observations will constrain computational models and direct the questions posed by them. Answers to questions such as the role of background electrolytes on the hydration and dehydration of ions in solution and at the mineral surface, or the differences in incorporation of elements from solution at different sites on a mineral surface, are likely to depend heavily on developments in molecular modelling.

The development of fully predictive models of how crystal growth can be modified and controlled by additives in solution has wide applications in fundamental science as well as industry. In the pharmaceutical industry, controlling crystal growth with additives is a vital, yet empirical, strategy. The prevention of crystal growth by inhibitors is similarly empirical, yet is a standard procedure in preventing scale formation in oil wells, in geothermal power plants, desalination plants, paper manufacturing, beer production and many other industrial processes. The growth of salts is the cause of degradation of porous building stone and various strategies are being developed to mitigate such damage. In all of these applications, AFM has an important role in developing a better understanding of the underlying mechanisms.

Understanding minor-element and trace-element incorporation during crystal growth will lead to better models of ion partitioning. The differences between adsorption and incorporation of different elements on different surface sites on a crystal will require a re-appraisal of concepts such as equilibrium partition coefficients. Our

knowledge of the nature of fluids in the crust is based on understanding the meaning of minor-element and trace-element compositions in minerals and how we can relate this to fluid compositions during crystal growth. A critical application of this is in the determination of past (and future) ocean climates and environments. Much of our understanding of the Earths climate history is based on interpretations of the chemical variability within calcium carbonate shells and skeletons of marine organisms. The elemental ratios (e.g. Mg/Ca, Sr/Ca, Ba/Ca, B/Ca) in biogenic and abiogenic carbonates are used to set up proxies to correlate these ratios with various aspects of palaeoenvironments including seawater temperature, composition, salinity, pH and hence atmospheric CO_2 concentration at the time of growth. However, without an understanding of the mechanism of incorporation, the role of fluid composition, background electrolytes and organic additives in solution, and the feedback between incorporation and growth mechanism, these empirical proxies and correlations will always be questionable. Atomic force microscopy will continue to play an important role in investigations in this area.

An obvious limitation of AFM is that, used alone, it cannot provide compositional information on the mineral surface, and element adsorption and incorporation is inferred from the subtle changes in surface and step-edge morphologies during *in situ* observations of crystal growth. Techniques based on measuring the forces between individual surface atoms and the AFM tip are being developed (Sugimoto *et al*., 2007) but this is limited to atomic scale resolution at cryogenic temperatures under high vacuum. Newly developed atomic force microscopes have the possibility of combining additional spectroscopic methods, such as Raman spectroscopy, and it is likely that with increased sensitivity such instruments will be able to be used in *in situ* growth experiments to identify new phases precipitating on the mineral surfaces under study.

Acknowledgements

The authors are grateful to many of the authors of the references listed here for their pioneering and inspiring research. Encarnación Ruiz-Agudo would like to acknowledge an Experienced Researcher Marie Curie Fellowship at the University of Münster, Germany, from 2009–2011 in the EU Initial Training Network Delta-Min (Mechanisms of Mineral Replacement Reactions) Grant PITN-GA-2008-215360, as well as financial support from the University of Granada, Spain (Plan Propio Program, Reintegration Grant) and the research group RNM-179 (Junta de Andaluc'a, Spain). The authors are most grateful to Frank Hawthorne for initiating this review paper for his careful and thorough review, which has improved the manuscript.

References

Arvidson, R.S., Ertan, I.E., Amonette, J.E., and Luttge, A. (2003) Variations in calcite dissolution rates: a fundamental problem? *Geochimica et Cosmochimica Acta*, **67**, 1623–1624.

Arvidson, R.S., Collier, M., Davis, K.J., Vinson, M.D., Amonette, J.E. and Luttge, A. (2006) Magnesium inhibition of calcite dissolution kinetics. *Geochimica et Cosmochimica Acta*, **70**, 583–594.

Astilleros, J.M., Pina, C.M., Fernández-Díaz, L. and Putnis, A. (2000) The effect of barium on calcite $(10\bar{1}4)$ surfaces during growth. *Geochimica et Cosmochimica Acta*, **64**, 2965–2972.

Astilleros, J.M., Pina, C.M., Fernández-Díaz, L. and Putnis, A. (2002) Molecular scale surface processes during the growth of calcite in the presence of manganese. *Geochimica et Cosmochimica Acta*, **66**, 3177–3189.

Astilleros, J.M., Pina, C.M., Fernández-Díaz, L. and Putnis, A. (2003) Nanoscale growth of solids crystallising from multicomponent aqueous solutions. *Surface Science*, **545**, L767–L773.

Astilleros, J.M., Fernández-Díaz, L. and Putnis, A. (2010) The role of magnesium in the growth of calcite: an AFM study. *Chemical Geology*, **271**, 52–58.

Binnig, G., Quate, C.F., Ginzton, E.L. (1986) Atomic force microscope. *Physical Review Letters*, **56**, 930–933

Bisschop, J., Dysthe, D.K., Putnis, C.V. and Jamtveit, B. (2006) In situ AFM study of the dissolution and recrystallization behaviour of polished and stressed calcite surfaces. *Geochimica et Cosmochimica Acta*, **70**, 1728–1738.

Buhmann, D. and Dreybrodt, W. (1987) Calcite dissolution kinetics in the system H_2O–CO_2–$CaCO_3$ with participation of foreign ions. *Chemical Geology*, **64**, 89–102.

Cabrera, N. and Vermilyea, D.A. (1958) The growth of crystals from solution. Pp. 393–410 in: *Growth and Perfection of Crystals* (R.H. Doremus, B.W. Roberts, D. Turnbull, editors). Wiley, New York, 609 pp.

Chada, V.G.R., Hausner, D.B., Strongin, D.R., Rouff, A.A. and Reeder, R.J. (2005) Divalent Cd and Pb

uptake on calcite {101$\bar{4}$} cleavage faces: An XPS and AFM study. *Journal of Colloid and Interface Science*, **288**, 350–360.

Chernov, A.A. (1984) *Modern Crystallography III*, Springer Series Solid State, Volume 36. Springer, Heidelberg, Germany.

Collins, K.D. (1997) Charge density-dependent strength of hydration and biological structure. *Biophysical Journal*, **72**, 65–76.

Compton, R.G. and Unwin, P.R. (1990) The dissolution of calcite in aqueous solution at pH < 4: kinetics and mechanism. *Philosophical Transactions of the Royal Society of London*, **A330**, 1–45.

Compton, R.G., Pritchard, K.L., Unwin, P.R., Grigg, G., Silvester, P., Lees, M. and House, W.A. (1989) The effect of carboxylic acids on the dissolution of calcite in aqueous solution. *Journal of Chemical Society, Faraday Transactions*, **185**, 4335–4366.

Cooke, D., Gray, R., Sand, K., Stipp, S. and Elliott, J. (2010) Interaction of ethanol and water with the {104} surface of calcite. *Langmuir*, **26**, 14520–14529.

Cubillas, P. and Higgins, S.R. (2009) Friction characteristics of Cd-rich carbonate films on calcite surfaces: implications for compositional differentiation at the nanometer scale. *Geochemical Transactions*, **10**, http://dx.doi.org/10.1186/1467-4866-10-7.

Davis, K.J., Dove, P.M. and De Yoreo, J.J. (2000) The role of Mg^{2+} as an impurity in calcite growth. *Science*, **290**, 1134–1137.

Davis, K.J., Dove, P.M., Wasylenki, L.E. and De Yoreo, J.J. (2004) Morphological consequences of differential Mg^{2+} incorporation at structurally distinct steps on calcite. *American Mineralogist*, **89**, 714–720.

De Giudici, G. (2002) Surface control *vs*. diffusion control during calcite dissolution: dependence of step-edge velocity upon solution pH. *American Mineralogist*, **87**, 1279–1285.

De Leeuw, N.H., Redfern, S.E., Cooke, D.J., Osguthorpe, D.J. and Parker, S.C. (2001) Modeling dynamic properties of mineral surfaces. *Solid–Liquid Interface Theory*, **8**, 97–112.

De Yoreo, J.J. and Dove, P.M. (2004) Shaping crystals with biomolecules. *Science*, **306**, 1301–1302.

De Yoreo, J.J. and Vekilov, P.G. (2003) Principles of crystal nucleation and growth. Pp. 57–93 in: *Biomineralization* (P.M. Dove, J.J. De Yoreo and S. Weiner, editors). Reviews in Mineralogy and Geochemistry, **54**. Mineralogical Society of America, Washington DC and the Geochemical Society, St Louis, Missouri, USA.

De Yoreo, J.J., Zepeda-Ruiz, L.A., Friddle, R.W., Qiu, S.R., Wasylenki, L.E., Chernov, A.A., Gilmer, G.H. and Dove, P.M. (2009) Rethinking classical crystal growth models through molecular scale insights: consequences of kink-limited kinetics. *Crystal Growth & Design*, **9**, 5135–5144.

Dove, P.M. and Hochella, M.F., Jr (1993) Calcite precipitation mechanisms and inhibition by orthophosphate: *in situ* observations by scanning force microscopy. *Geochimica et Cosmochimica Acta*, **57**, 705–714.

Dove, P.M. and Platt, F.M. (1996) Compatible real-time rates of mineral dissolution by atomic force microscopy (AFM). *Chemical Geology*, **127**, 331–338.

Dove, P.M., De Yoreo, J.J., Davis, K.J. (2004) Inhibition of $CaCO_3$ crystallization by small molecules: the magnesium example. Pp. 55–82 in: *From Solid–Fluid Interfaces to Nanostructural Engineering, Volume II: Assembly in hybrid and biological systems*, (X.Y. Liu and J.J. De Yoreo, editors). Kluewer Academic Publishers, New York.

Duckworth, O.W. and Martin, S.T. (2004) Dissolution rates and pit morphologies of rhombohedral carbonate minerals. *American Mineralogist*, **89**, 554–563.

Eldhadj, S., De Yoreo, J.J., Hoyer, J.R. and Dove, P.M. (2006*a*) Role of molecular charge and hydrophilicity in regulating the kinetics of crystal growth. *Proceedings of the National Academy of Sciences*, **103**, 19237–19242.

Eldhadj, S., Salter, E.A., Wierzbicki, A., De Yoreo, J.J., Han, N. and Dove, P.M. (2006*b*) Peptide controls on calcite mineralization: polyaspartate chain length affects growth kinetics and acts as a stereochemical switch on morphology. *Crystal Growth & Design*, **6**, 197–201.

Freij, S.J., Putnis, A. and Astilleros, J.M. (2004) Nanoscale observations of the effect of cobalt on calcite growth and dissolution. *Journal of Crystal Growth*, **267**, 288–300.

Freij, S.J., Godelitsas, A. and Putnis, A. (2005) Crystal growth and dissolution processes at the calcite–water interface in the presence of zinc ions. *Journal of Crystal Growth*, **273**, 535–545.

Glynn, P.D. and Reardon, E.J. (1990) Solid-solution aqueous-solution equilibria: thermodynamic theory and representation. *American Journal of Science*, **290**, 164–201.

Godelitsas, A., Astilleros, J.M., Hallam, K.R., Löns, J., and Putnis, A. (2003) Microscopic and spectroscopic investigation of the calcite surface interacted with Hg(II) in aqueous solutions. *Mineralogical Magazine*, **67**, 1193–1204

Gratz, A.J., Hillner, P.E. and Hansma, P.K. (1993) Step dynamics and spiral growth on calcite. *Geochimica et Cosmochimica Acta*, **57**, 491–495.

Gutjahr, A., Dabringhaus, H. and Lacmann, R. (1996) Studies of the growth and dissolution kinetics of the $CaCO_3$ polymorphs calcite and aragonite I. Growth

and dissolution rates in water. *Journal of Crystal Growth*, **158**, 296–309.

Harstad, A.O. and Stipp, S.L.S. (2007) Calcite dissolution: effects of trace cations naturally present in Iceland spar calcites. *Geochimica et Cosmochimica Acta*, **71**, 56–70.

Hay, M.B., Workman, R.K. and Manne, S. (2003) Mechanisms of metal ion sorption on calcite: composition mapping by lateral force microscopy. *Langmuir*, **19**, 3727–3740.

Henriksen, K., Stipp, S.L.S., Young, J.R. and Marsh, M.E. (2004) Biological control on calcite crystallization: AFM investigation of coccolith polysaccharide function. *American Mineralogist*, **89**, 1709–1716.

Hillner, P.E., Gratz, A.J., Manne, S. and Hansma, P.K. (1992) Atomic scale imaging of calcite growth and dissolution in real time. *Geology*, **20**, 359–362.

Hillner, P.E., Manne, S., Hansma, P.K. and Gratz, A.J. (1993) Atomic force microscope: a new tool for imaging crystal growth processes. *Faraday Discussions*, **95**, 191–197.

Hoch, A.R., Reddy, M.M. and Aiken, G.R. (2000) Calcite crystal growth inhibition by humic substances with emphasis on hydrophobic acids from the Florida Everglades. *Geochimica et Cosmochimica Acta*, **64**, 61–72.

Hochella, M.F., Jr, Eggleston, C.M., Elings, V.B. and Thompson, M.S. (1990) Atomic structure and morphology of the albite (010) surface: an atomic-force microscope and electron diffraction study. *American Mineralogist*, **75**, 7–8.

Hoffmann, U. and Stipp, S.L.S. (2001) The behaviour of Ni^{2+} on calcite surfaces. *Geochimica et Cosmochimica Acta*, **65**, 4131–4139.

Jordan, G. and Ramennensee, W. (1998) Dissolution rates of calcite ($10\bar{1}4$) obtained by scanning force microscopy: microtopography-based dissolution kinetics on surfaces with anisotropic step velocities. *Geochimica et Cosmochimica Acta*, **62**, 941–947.

Kamiya, N., Kagi, H., Tsunomori, F., Tsuno, H, Notsu, K. (2004) Effect of trace lanthanum ion on dissolution and crystal growth of calcium carbonate. *Journal of Crystal Growth*, **267**, 635–645.

Kim, R., Kim, C., Lee, S., Kim, J. and Kim, I. (2009) *In situ* atomic force microscopy study on the crystallization of calcium carbonate modulated by poly(vinyl alcohol)s. *Crystal Growth and Design*, **9**, 4584–4587.

Kowacz, M. and Putnis, A. (2008) The effect of specific background electrolytes on water structure and solute hydration: consequences for crystal dissolution and growth. *Geochimica et Cosmochimica Acta*, **72**, 4476–4487.

Kowacz, M., Putnis, C.V. and Putnis, A. (2007) The effect of cation:anion ratio in solution on the mechanism of barite growth at constant supersaturation: role of the desolvation process on the growth kinetics. *Geochimica et Cosmochimica Acta*, **71**, 5168–5179.

Kubota, N. and Mullin, J.W. (1995) A kinetic model for crystal growth from aqueous solution in the presence of impurity. *Journal of Crystal Growth*, **152**, 203–208.

Lardge, J.S., Duffy, D.M., Gillan, M.J., Watkins, M. (2010) *Ab initio* simulations of the interaction between water and defects on the calcite ($10\bar{1}4$) surface. *Journal of Physical Chemistry C*, **114**, 2664–2668.

Larsen, K., Bechgaard, K. and Stipp, S.L.S. (2010) The effect of the Ca^{2+} to CO_3^{2-} activity ratio on spiral growth at the calcite $\{10\bar{1}4\}$ surface. *Geochimica et Cosmochimica Acta*, **74**, 2099–2109.

Lasaga, A.C. and Lüttge, A. (2001) Variation of crystal dissolution rate based on a dissolution stepwave model. *Science*, **291**, 2400–2404.

Lea, A.S., Amonette, J.E., Baer, D.R., Liang, Y. and Colton, N.G. (2001) Microscopic effects of carbonate, manganese and strontium ions on calcite dissolution. *Geochimica et Cosmochimica Acta*, **65**, 369–379.

Lea, A.S., Hurt, T.T., El-Azab, A., Amonette, J.E. and Baer, D.R. (2003) Heteroepitaxial growth of a manganese carbonate secondary nano-phase on the ($10\bar{1}4$) surface of calcite in solution. S*urface Science*, **524**, 63–77.

Li, M. and Mann, S. (2002) Emergent nanostructures: water-induced mesoscale transformation of surfactant-stabilized amorphous calcium carbonate nanoparticles in reverse microemulsions. *Advanced Functional Materials*, 12, 773–779.

Liang, Y. and Baer, D.R. (1997) Anisotropic dissolution at the $CaCO_3$ ($10\bar{1}4$)-water interface. *Surface Science*, **373**, 275–287.

Liang, Y., Baer, D.R., McCoy, J.M., Amonette, J.E. and LaFemina, J.P. (1996*a*) Dissolution kinetics at the calcite-water interface. *Geochimica et Cosmochimica Acta*, **60**, 4883–4887.

Liang Y., Baer, D.R., McCoy, J.M., Amonette, J.E. and LaFemina, J.P. (1996*b*) Interplay between step velocity and morphology during the dissolution of $CaCO_3$ surface. *Journal of Vacuum Science and Technology A*, **14**, 1368–1375.

Lüttge, A. (2005) Etch pit coalescence, surface area, and overall mineral dissolution rates. *American Mineralogist*, **90**, 1776–1783.

Lüttge A., Winkler, U. and Lasaga, A.C. (2003) Interferometric study of the dolomite dissolution: a new conceptual model for mineral dissolution. *Geochimica et Cosmochimica Acta*, **67**, 1099–1116.

MacInnis, I.N. and Brantley, S.L. (1992) The role of dislocations and surface morphology in calcite

dissolution. *Geochimica et Cosmochimica Acta*, **56**, 1113–1126.

Marti, O., Drake, B., Hansma, P. K. (1987) Atomic force microscopy of liquid-covered surfaces: atomic resolution images. *Applied Physics Letters*, **51**, 484–486.

McCoy, J.M. and LaFemina, J.P. (1997) Kinetic Monte Carlo investigation of pit formation at the $CaCO_3$ $(10\bar{1}4)$ surface–water interface. *Surface Science*, **373**, 288–299.

Morse, J.W. and Arvidson, R.S. (2002) The dissolution kinetics of major sedimentary carbonate minerals. *Earth-Science Reviews*, **58**, 51–84.

Nehrke, G., Reichart, G.J., Van Cappellen, P., Meile, C. and Bijma, J. (2007) Dependence of calcite growth rate and Sr partitioning on solution stoichiometry: non-Kossel crystal growth. *Geochimica et Cosmochimica Acta*, **71**, 2240–2249.

Nilsson, O. and Sternbeck, J. (1999) A mechanistic model for calcite crystal growth using surface speciation. *Geochimica et Cosmochimica Acta*, **63**, 217–225.

Oelkers, E.H., Golubev, S.V., Pokrovsky, O.S. and Benezeth, P. (2011) Do organic ligands affect calcite dissolution rates? *Geochimica et Cosmochimica Acta*, **75**, 1799–1813.

Ohnesorge, F., and Binnig, G. (1993) True atomic resolution by atomic force microscopy through repulsive and attractive forces. *Science*, **260**, 1451.

Orme, C.A., Noy, A., Wierzbicki, A., McBride, M.T., Grantham, M., Teng, H.H., Dove, P.M. and De Yoreo, J.J. (2001) Formation of chiral morphologies through selective binding of amino acids to calcite surface steps. *Nature*, **411**, 775–779

Paquette, J. and Reeder, R.J. (1995) Relationship between surface structure, growth mechanism, and trace element incorporation in calcite. *Geochimica et Cosmochimica Acta*, **59**, 735–749.

Parkhurst D.L. and Appelo C.A.J. (1999) *Users guide to PHREEQC (version 2) – A Computer Program for Speciation, Batch Reaction, One Dimensional Transport, and Inverse Geochemical Calculations*. U.S. Geological Survey Water-Resources Investigation Report 99–4259, 312pp.

Perdikouri, C., Putnis, C.V., Kasioptas, A. and Putnis, A. (2009) An atomic force microscopy study of the growth of a calcite surface as a function of calcium/total carbonate concentration ratio in solution at constant supersaturation. *Crystal Growth & Design*, **9**, 4344–4350.

Perez-Garrido, C., Fernández-Díaz, L., Pina, C.M. and Prieto, M. (2007) In situ AFM observations of the interaction between calcite surfaces and Cd-bearing aqueous Solutions. *Surface Science*, **601**, 5499–5509.

Piana, S., Jones, F. and Gale, J.D. (2006) Assisted desolvation as a key kinetic step for crystal growth. *Journal of the American Chemical Society*, **128**, 13568–13574.

Pina, C.M., Becker, U., Risthaus, P., Bosbach, D. and Putnis, A. (1998) Molecular-scale mechanisms of crystal growth in barite. *Nature*, **395**, 483–486.

Plummer, L.N., Wigley, T.M.L. and Parkhurst, D.L. (1978) The kinetics of calcite dissolution in CO_2–water systems at 5ºC to 60ºC and 0.0 to 1.0 atm CO_2. *American Journal of Science*, **278**, 179–216.

Pokrovsky, O.S. and Schott, J. (2002) Surface chemistry and dissolution kinetics of divalent metal carbonates. *Environmental Science and Technology*, **36**, 426–432.

Prieto, M. (2009) Thermodynamics of Solid Solution–Aqueous Solution Systems. Pp. 47–85 in: *Thermodynamics and Kinetics of Water–Rock Interaction* (E.H. Oelkers and J. Schott, editors). Reviews in Mineralogy & Geochemistry, **70**. Mineralogical Society of America, Washington DC and the Geochemical Society, St Louis, Missouri, USA.

Qiu, S.R. and Orme, C.A. (2008) Dynamics of biomineral formation at the near-molecular level. *Chemical Reviews*, **108**, 4784–4822

Rachlin, A.L., Henderson, G.S. and Goh, M.C. (1992) An atomic force microscope (AFM) study of the calcite cleavage plane: image averaging in Fourier space. *American Mineralogist*, **77**, 904–910.

Rashkovich, L.N., De Yoreo, J.J., Orme, C.A. and Chernov, A.A. (2006) In situ atomic force microscopy of layer-by-layer crystal growth and key growth concepts. *Crystallography Reports*, **51**, 1063–1074.

Reeder, R.J. (1996) Interaction of divalent cobalt, zinc, cadmium, and barium with the calcite surface during layer growth. *Geochimica et Cosmochimica Acta*, **60**, 1543–1552.

Ruiz-Agudo, E., Putnis, C.V., Jiménez-López, C. and Rodríguez-Navarro, C. (2009) An AFM study of calcite dissolution in concentrated saline solutions: the role of magnesium ions. *Geochimica et Cosmochimica Acta*, **73**, 3201–3217.

Ruiz-Agudo, E., Di Tommaso, D., Putnis, C.V., de Leeuw, N.H. and Putnis, A. (2010*a*) Interactions between organophosphonate-bearing solutions and (104) calcite surfaces: an atomic force microscopy and first-principles molecular dynamics study. *Crystal Growth & Design*, **10**, 3022–3035.

Ruiz-Agudo, E., Kowacz, M., Putnis, C.V. and Putnis, A. (2010*b*) The role of background electrolytes on the kinetics and mechanism of calcite dissolution. *Geochimica et Cosmochimica Acta*, **74**, 1256–1267.

Ruiz-Agudo, E., Putnis, C.V., Rodriguez-Navarro, C., Putnis, A. (2011*a*) Effect of pH on calcite growth at constant $a_{Ca^{2+}}/a_{CO_3^{2+}}$ and supersaturation.

Geochimica et Cosmochimica Acta, **75**, 284–296.

Ruiz-Agudo, E., Putnis, C.V., Wang L.J. and Putnis, A. (2011*b*) Specific effects of background electrolytes on the kinetics of step propagation during calcite growth. *Geochimica et Cosmochimica Acta*, **75**, 3803–3814.

Ruiz-Agudo, E., Urosevic, M., Putnis, C.V., Rodriguez-Navarro, C., Cardell, C., Putnis, A. (2011*c*) Ion-specific effects on the kinetics of crystal dissolution. *Chemical Geology*, **281**, 364–371.

Sand, K., Yang, M., Makovicky, E., Cooke, D., Hassenkam, T., Bechgaard, K. and Stipp, S. (2010) Binding of ethanol on calcite: the role of the OH bond and its relevance to biomineralization. *Langmuir*, **26**, 15239–15247.

Schott, J., Brantley, S., Crerar, D., Guy, C., Borcsik, M. and Willaime, C. (1989) Dissolution kinetics of strained calcite. *Geochimica et Cosmochimica Acta*, **53**, 373–382.

Sethmann, I., Putnis, A., Grassmann, O. and Lobmann, P. (2005) Observation of nano-clustered calcite growth via an amorphous transient phase mediated by organic polyanions: a close match for biomineralization. *American Mineralogist*, **90**, 1213–1217.

Shiraki, R., Rock, P.A. and Casey, W.H. (2000) Dissolution kinetics of calcite in 0.1 M NaCl solution at room temperature: an atomic force microscopic (AFM) study. *Aquatic Geochemistry*, **6**, 87–108.

Sjöberg, E.L. and Rickard, D.T. (1984) Calcite dissolution kinetics: surface speciation and the origin of the variable pH dependence. *Chemical Geology*, **42**, 119–136.

Stack, A.G. and Grantham, M.C. (2010) Growth rate of calcite steps as a function of aqueous calcium-to-carbonate ratio: independent attachment and detachment of calcium and carbonate ions. *Crystal Growth & Design*, **10**, 1409–1413.

Stephenson, A.E., Wu, L., Wu, K.J., Hoyer, J.D., De Yoreo, J.J. and Dove, P.M. (2008) Peptides enhance Mg contents in calcite: insights to origins of vital effects. *Science*, **322**, 274–277.

Sternbeck, J. (1997) Kinetics of rhodochrosite crystal growth at 25ºC: the role of surface speciation. *Geochimica et Cosmochimica Acta*, **61**, 785–793.

Stipp, S.L.S. (1999) Toward a conceptual model of the calcite surface: hydration, hydrolysis and surface potential. *Geochimica et Cosmochimica Acta*, **63**, 3121–3131.

Stipp, S.L. and Hochella, M.F., Jr (1991) Structure and bonding environments at the calcite surface as observed with X-ray photoelectron spectroscopy (XPS) and low-energy electron diffraction (LEED). *Geochimica et Cosmochimica Acta*, **55**, 1723–1736.

Stipp, S.L.S, Eggleston, C.M. and Nielsen, B.S. (1994) Calcite surface structure observed at micro-topographic and molecular scale with atomic force microscopy (AFM). *Geochimica et Cosmochimica Acta*, **58**, 3023–3033.

Sugimoto, Y., Pou, P., Abe, M., Jelinek, P., Pérez, R., Morita, S. and Custance, O. (2007) Chemical identification of individual surface atoms by atomic force microscopy. *Nature*, **446**, 64–67.

Sunagawa, I. (1987) *Morphology of Crystals*. Terra Science Publications, Tokyo.

Teng, H.H. (2004) Control by saturation state on etch pit formation during calcite dissolution. *Geochimica et Cosmochimica Acta*, **68**, 253–262.

Teng, H.H. and Dove, P.M. (1997) Surface site-specific interactions of aspartate with calcite during dissolution: implications for biomineralization. *American Mineralogist*, **82**, 878–887.

Teng, H.H., Dove, P.M. and De Yoreo, J.J. (1999) Reversed calcite morphologies induced by microscopic growth kinetics: insight into biomineralization. *Geochimica et Cosmochimica Acta*, **63**, 2507–2512.

Teng, H.H., Dove, P.M. and De Yoreo, J.J. (2000) Kinetics of calcite growth: surface processes and relationships to macroscopic rate laws. *Geochimica et Cosmochimica Acta*, **64**, 2255–2266.

Teng, H.H. Chen, Y. and Pauli, E. (2006) Direction specific interactions of 1,4-dicarboxcylic acid with calcite surfaces. *Journal of American Chemical Society*, **128**, 14482–14484.

Tesoriero, A.J. and Pankow, J.F. (1996) Solid solution partitioning of Sr^{2+}, Ba^{2+}, and Cd^{2+} to calcite. *Geochimica et Cosmochimica Acta*, **60**, 1053–1063.

Treccani, L., Mann K., Heinemann F. and Fritz, M. (2006) Perlwapin, an abalone nacre protein with three fourdisulfide core (whey acidic protein) domains, inhibits the growth of calcium carbonate crystals. *Biophysical Journal*, **91**, 2601–2608.

Urosevic, M., Rodr'guez-Navarro, C.M., Putnis, C.V., Cardell, C., Putnis, A. and Ruiz-Agudo, E. (2012) In situ, nanoscale observations of the dissolution of $(10\bar{1}4)$ dolomite cleavage surfaces, *Geochimica et Cosmochimica Acta*, **80**, 1–13.

van Enckevort, W.J.P., van den Berg, A.C.J.F., Kreuwel, K.B.G. Derksen, A.J. and Couto, M.S. (1996) Impurity blocking of growth steps: experiments and theory. *Journal of Crystal Growth*, **166**, 156–161.

Vavouraki, A.I., Putnis, C.V., Putnis, A. and Koutsoukos, P. (2008) An atomic force microscopy study of the growth of calcite in the presence of sodium sulfate. *Chemical Geology*, **253**, 243–251.

Vavouraki, A.I., Putnis, C.V., Putnis, A. and Koutsoukos, P. (2010) Crystal growth and dissolution of calcite in the presence of fluoride ions: an atomic force microscopy study. *Crystal Growth & Design*, **10**, 60–69.

Vinson, M.D. and Luttge, A. (2005) Multiple length-scale kinetics: an integrated study of calcite

dissolution rates and strontium inhibition. *American Journal of Science*, **305**, 119–146.

Vinson, M.D., Arvidson, R.S. and Luttge, A. (2007) Kinetic inhibition of calcite (104) dissolution by aqueous manganese (II). *Journal of Crystal Growth*, **307**, 116–125.

Walters, D.A., Smith, B.L., Belcher, A.M., Paloczi, G.T. Stucky, G.D., Morse, D.E. and Hansma, P.K. (1997) Modification of calcite crystal growth by abalone shell proteins: an atomic force microscope study. *Biophysical Journal*, **72**, 1425–1433.

Wang, L.J., Ruiz-Agudo, E., Putnis, C.V., Putnis, A. (2011) Direct observations of the modification of calcite growth morphology by Li+ through selectively stabilizing energetically unfavourable faces. *ChemEngComm*, **13**, 3962–3966

Wasylenki, L.E., Dove, P.M. and De Yoreo, J.J. (2005*a*) Effects of temperature and transport conditions on calcite growth in the presence of Mg^{2+}: Implications for paleothermometry. *Geochimica et Cosmochimica Acta* **69**, 4227–4236.

Wasylenki L.E., Dove P.M. Wilson D.S. and Yoreo J.J.D. (2005*b*) Nanoscale effects of strontium on calcite growth: an in situ AFM study in the absence of vital effects. *Geochimica et Cosmochimica Acta*, **69**, 3017–3027.

Weiner, S. (1979) Aspartic acid-rich proteins: major components of the soluble organic matrix of mollusk shells. *Calcified Tissue International*, **29**, 163–167.

Wierzbicki, A., Sikes, C.S,. Madura, J.D. and Drake, B. (1994) Atomic force microscopy and molecular modeling of protein and peptide binding to calcite. *Calcified Tissue International*, **54**, 133–141.

Xu, M. and Higgins, S.R. (2011) Effects of magnesium ions on near-equilibrium calcite dissolution: step kinetics and morphology. *Geochimica et Cosmochimica Acta*, **75**, 719–733

Xu, M., Hu, X., Knauss, K.G. and Higgins, S.R. (2010) Dissolution kinetics of calcite at 50–70ºC: an atomic force microscopic study under near-equilibrium conditions. *Geochimica et Cosmochimica Acta*, **74**, 4285–4297.

Yang, M., Stipp, S.L.S. and Harding, J. (2008) Biological control on calcite crystallization by polysaccharides. *Crystal Growth & Design*, **8**, 4066–4074.

Zhang, J. and Nancollas, G.H. (1998) Kink density and rate of step movement during growth and dissolution of an AB crystal in a nonstoichiometric solution, *Journal of Colloid and Interface Science*, **200**, 131–145.

Zuddas, P. and Mucci, A. (1998) Kinetics of calcite precipitation from seawater: II. The influence of the ionic strength. *Geochimica et Cosmochimica Acta*, **62**, 757–766.